

Pia Benedikt, BSc

# **Cloning, Expression and Characterization of PEDF**

## **MASTER'S THESIS**

to achieve the university degree of

Master of Science

Master's degree programme: Biochemistry and Molecular Biomedical Sciences

submitted to

**Graz University of Technology**

Supervisor

Priv.-Doz. Mag. Dr. Martina Schweiger

Institute of Molecular Biosciences

Graz, April 2015

## **AFFIDAVIT**

I declare that I have authored this thesis independently, that I have not used other than the declared sources/resources, and that I have explicitly indicated all material which has been quoted either literally or by content from the sources used. The text document uploaded to TUGRAZonline is identical to the present master's thesis dissertation.

---

Date

---

Signature

## **Danksagung**

Zunächst möchte ich mich an dieser Stelle bei all denjenigen bedanken, die mich während der Anfertigung meiner Master-Arbeit unterstützt und immer wieder aufs Neue motiviert haben.

Ganz besonderer Dank gilt hierbei Priv. Doz. Dr. Martina Schweiger, die mich während meiner gesamten Masterarbeit an diesem Institut betreut hat. Vor allem danke ich Ihr für die warmherzige Betreuung und Unterstützung in allen Situationen. Durch ihre herausragende Expertise konnte sie mich immer wieder bei meinen Fragen unterstützen und neue Anregungen geben. Des Weiteren möchte ich mich auch bei den anderen Mitgliedern der Zechner AG bedanken, die jederzeit für Fragen zur Verfügung standen. Es war immer ein Vergnügen mit euch zusammen zu arbeiten.

Zusätzlich möchte ich mich auch noch bei Lisa, Ursula, Sabrina und Nadja bedanken, die meinen Sorgen immer ein Gehör schenkten ohne es Leid zu werden. Ohne euch wäre die Zeit nicht dieselbe gewesen. Darüber hinaus möchte ich meinen Eltern danken, die mich in jeder Situation meines Lebens unterstützt haben, auch wenn es vielleicht manchmal schwer fiel. Ein spezieller Dank gilt meinem Lebenspartner Robin, ohne dich wäre ich nicht der Mensch der ich heute bin.

## Abstract

Pigment epithelium-derived factor (PEDF) is a 50 kDa adipokine, belonging to the serine protease inhibitor family. PEDF was first identified as a factor secreted from human retinal epithelial cells with neurotrophic and neuroprotective functions. Besides these functions PEDF is also known to suppress cancer growth by the activation of the apoptotic cascade, the inhibition of angiogenesis and the induction of differentiation. Previous studies reported that PEDF is upregulated in individuals with metabolic syndrome and type 2 diabetes. Although PEDF is best known for its anti-cancer effects, recent work has implicated PEDF in the development of obesity-related insulin resistance. PEDF is thought to exert its biological action by binding to cell surface receptors. Interestingly, adipose triglyceride lipase (ATGL) was recently identified as a receptor with phospholipase A<sub>2</sub> (PLA) activity. *Notari et al.* hypothesized that binding of PEDF to ATGL stimulates its PLA activity, which leads to the release of free fatty acids (FFAs) and lysophospholipids. Further publications also proposed an intracellular pro-lipolytic effect of PEDF through binding to ATGL, facilitating the translocation onto lipid droplets for triglyceride (TG) degradation. However, so far it is not clear how PEDF exerts its pro-lipolytic function. Hence, the aim of my study was to investigate the role of PEDF in lipid metabolism in more detail.

Despite the missing potential to stimulate TG hydrolase and PLA activity *in vitro*, PEDF significantly increased basal and stimulated lipolysis in differentiated 3T3-L1 cells. In addition to PEDFs binding to ATGL, co-immunoprecipitation studies revealed an interaction with the co-activator protein CGI-58. The incubation of differentiated 3T3-L1 cells with PEDF containing medium caused an increase in FFA release. Furthermore, western blot analysis indicates that PEDFs effect depends on a ligand-receptor mechanism, involving the cAMP dependent signalling cascade.

## Zusammenfassung

Pigment epithelium-derived factor (PEDF) ist ein 50 kDa Adipokin, der Serinprotease-Inhibitor Familie. PEDF wurde als ein Faktor mit neurotrophen und neuroprotektiven Funktionen identifiziert, welcher von humanen Epithelzellen der Retina sekretiert wird. Zudem ist PEDF auch bekannt für die Unterdrückung des Krebswachstums durch Aktivierung der apoptotischen Kaskade, Inhibierung der Angiogenese und durch Induktion der Differenzierung. Neue Studien berichteten, dass PEDF bei Personen mit metabolischem Syndrom und Typ 2 Diabetes hochreguliert ist. Obwohl PEDF am besten bekannt ist für seine Anti-Krebswirkung, zeigten neueste Studien auch einen Zusammenhang zwischen PEDF und der Entwicklung von Adipositas-abhängiger Insulinresistenz. Dabei nimmt man an, dass PEDF seine Wirkung durch Bindung an Rezeptoren vermittelt. Überraschenderweise wurde kürzlich die Adipozyten-Triglycerid-Lipase (ATGL) als ein Rezeptor mit Phospholipase (PLA)-Aktivität identifiziert. *Notari et al.* nehmen an, dass die Bindung von PEDF an ATGL zu einer Stimulation der PLA-Aktivität führt, wodurch Fettsäuren (FS) und Lysophospholipide freigesetzt werden. Weitere Publikationen schlugen auch einen intrazellulären Effekt von PEDF durch Bindung an ATGL vor, wodurch die Translokation zu den Lipidtropfen und der Abbau von Triglyceriden (TG) erleichtert wird. Daher war das Ziel meiner Studie, die Rolle von PEDF im Lipidstoffwechsel genauer zu beleuchten.

Trotz der fehlenden Stimulation der TG-Hydrolase und PLA-Aktivität *in vitro*, führte PEDF in 3T3-L1 Zellen zu einer signifikanten Zunahme der basalen und stimulierten Lipolyse. Zusätzlich zur Bindung an ATGL, offenbarte die Co-Immunopräzipitation eine Interaktion mit CGI-58. Die Inkubation von differenzierten 3T3-L1 Zellen mit PEDF enthaltenem Medium führte zu einer Zunahme der FS-Freisetzung. Darüber hinaus lassen Western-Blot Analysen vermuten, dass der Wirkungsmechanismus von PEDF Rezeptor-abhängig ist und die cAMP-abhängige Signalkaskade beinhaltet.

# List of contents

<b>AFFIDAVIT</b>	<b>ii</b>
<b>Danksagung</b>	<b>iii</b>
<b>Abstract</b>	<b>iv</b>
<b>1. Introduction</b>	<b>1</b>
1.1. Adipose Tissue - a multifunctional organ	2
1.2. Lipolysis - lipases and co-regulators	3
1.2.1. ATGL	4
1.2.2. CGI-58	5
1.3. Hormonal regulation of lipolysis	7
1.3.1. Catecholamines	7
1.3.2. Insulin	8
1.4. PEDF	10
1.4.1. PEDF and ATGL	12
1.5. Aim of this thesis	14
<b>2. Materials</b>	<b>15</b>
2.1. Media	16
2.2. Buffers and Solutions	17
2.3. Primers	21
2.4. Vectors	22
2.5. Bacterial strains	24
2.6. Cell lines	24
2.7. Antibodies	26
2.8. Kits	27
<b>3. Methods</b>	<b>28</b>
3.1. Cloning	29
3.1.1. Polymerase chain reaction (PCR)	29
3.1.2. Gel electrophoresis	30
3.1.3. Restriction digest	31
3.1.4. Dephosphorylation of the vector	31
3.1.5. Phenol-Chloroform extraction	31
3.1.6. Ligation	32
3.1.7. Transformation	32
3.1.8. Small scale plasmid isolation - Miniprep	33
3.1.9. Large scale plasmid isolation - Maxiprep	33

3.1.10. Sequencing of the isolated DNA	33
3.2. General information about lentivirus generation	34
3.2.1. Transfection of HEK-293 packaging cells	35
3.2.2. Transduction of 3T3-L1 cells	35
3.2.3. Selection and cultivation	36
3.2.4. Induction of the Tet-off system	36
3.3. Cell culture	36
3.3.1. Cultivation of cells	36
3.3.2. Differentiation of 3T3-L1 preadipocytes	37
3.3.3. Transfection and preparation of cell lysates	37
3.4. Measuring Protein content	38
3.4.1. BCA protein assay	38
3.4.2. Bradford protein assay	39
3.4.3. SDS-PAGE	39
3.5. Expression analysis	40
3.5.1. Western blot analysis	40
3.6. Co-Immunoprecipitation	40
3.7. Assays	42
3.7.1. <i>In vitro</i> assay for triglyceride hydrolase activity	42
3.7.2. <i>In vitro</i> assay for phospholipase activity	42
3.7.3. Measurement of free fatty acids and glycerol release of cultured cells	43
3.7.4. Preparation of conditioned media containing PEDF	44
3.8. Statistical analysis	44
<b>4. Results</b>	<b>45</b>
4.1. New potential interaction partner of PEDF	46
4.2. Determination of TG hydrolase activity	49
4.3. Determination of phospholipase activity	54
4.4. PEDF secretion	55
4.5. Incubation of 3T3-L1 cells with PEDF containing medium	57
4.6. Effect of PEDF expression on differentiated 3T3-L1 cells	59
4.7. Western blot analysis of key enzymes in lipolysis	62
<b>5. Discussion</b>	<b>65</b>
<b>I. Abbreviations</b>	<b>70</b>
<b>II. References</b>	<b>72</b>
<b>III. List of figures</b>	<b>80</b>



# 1. Introduction

---

## **1.1. Adipose Tissue - a multifunctional organ**

Adipose tissue (AT) is the main energy reservoir in the human body and a major source of metabolic fuel (Lafontan & Langin 2009). Most of the energy reserves are stored within fat cells (adipocytes) of the AT, where dietary lipids are taken up and esterified to triglycerides (TGs) within specialized organelles, called lipid droplets (LDs). In times of high energy demand, when mobilization of endogenous energy is required, TGs are hydrolyzed by the coordinated process of lipolysis and released into the circulation as free fatty acids (FFAs) (Nielsen et al. 2014). These FFAs are then transported to peripheral tissues where they can serve as substrates for  $\beta$ -oxidation and ATP production (Kolditz & Langin 2010). Besides their function as energy substrates, FFAs are also essential precursors for all lipid classes, including those forming biological membranes. In addition, they are important for the regulation of protein function in acylated proteins and as ligands for nuclear receptor transcription factors (Zechner et al. 2009).

AT has long been seen exclusively as an energy storing organ. Apart from its active role in energy homeostasis and cellular signalling, it is now also recognized as the body's largest endocrine organ secreting numerous signalling molecules termed adipokines (Kershaw & Flier 2014). Dysfunctional AT is associated with increased infiltration and activation of immune cells, increased lipolysis and elevated free FFAs. Increased plasma levels of FFA lead to ectopic lipid deposition in skeletal muscle and liver followed by systemic insulin resistance and type II diabetes (Gustafson et al. 2009, Crowe et al. 2009). For this reason the AT is essential for the regulation of whole body fatty acid metabolism and insulin action (Borg et al. 2011).

The predominant type of AT in mammals is the white adipose tissue (WAT), which is mainly comprised of adipocytes, surrounded by loose connective tissue. The surrounding tissue is highly vascularized and innervated, contains macrophages, fibroblasts, lymph nodes, immune cells, adipocyte precursors, and other cell types. Among the metabolically relevant tissues, WAT is the most plastic organ and is mainly represented by the subcutaneous and visceral fat depots (Masoodi et al. 2014, Smorlesi et al. 2012).

White adipocytes are characterized by a unilocular lipid droplet, a thin rim of cytoplasm and nucleus and primarily act as storage cells for neutral lipids. Additionally, white fat cells also contribute to whole body insulation and have endocrine functions, which includes the secretion of adipokines such as leptin, adiponectin and pigment epithelium-derived factor (PEDF) (Rosenwald & Wolfrum 2014).

In contrast, brown adipose tissue (BAT) represents the major site for heat production (thermogenesis) and contributes to the ability of the body to defend against cold environmental temperatures (Cannon & Nedergaard 2004). In addition to multilocular LDs for TG storage, brown adipocytes display a high mitochondrial density (Cinti 2001). These BAT mitochondria are characterized by the unique presence of uncoupling protein 1 (UCP1), which is located in the inner mitochondrial membrane, where it uncouples the respiratory chain from ATP production through the translocation of protons into the mitochondrial matrix. Consequently, the energy preserved in the proton gradient is dissipated as heat (Klingenspor 2003). Because of its high vascularization, BAT is sufficiently provided with substrates and oxygen and the produced heat is efficiently distributed within the whole body (Cannon & Nedergaard 2004).

## **1.2. Lipolysis - lipases and co-regulators**

Lipolysis is defined as the sequential hydrolysis of TGs into FFAs and glycerol by a class of hydrolytic enzymes, commonly known as lipases. In this catabolic process, three lipases act in a coordinated manner to catalyze the release of one FFA in each step. Adipose triglyceride lipase (ATGL) is the rate-limiting enzyme in this lipolytic pathway and converts TGs to diglycerides (DGs) (Zimmermann et al. 2004). DGs are then further hydrolyzed to monoglycerides (MGs) by hormone-sensitive lipase (HSL) (Haemmerle et al. 2002), and monoglyceride lipase (MGL) cleaves MGs into glycerol and FFAs (Fredrikson 1986).

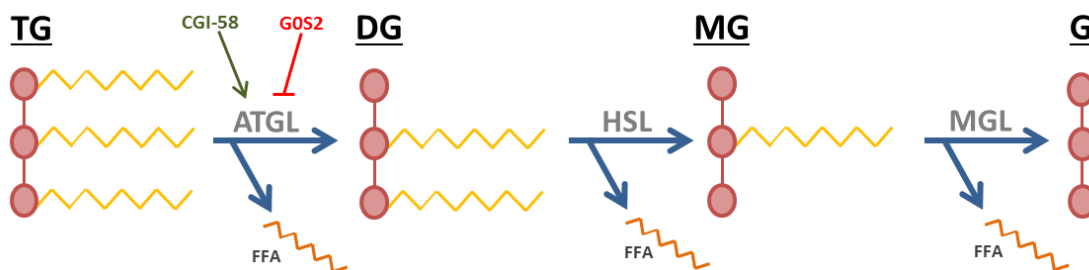


**Figure 1: Schematic illustration of lipolysis.** TGs are hydrolyzed by the sequential enzymatic action of ATGL, HSL and MGL, resulting in the release of one FFA in each step. In this process TGs are successively converted to DGs, then to MGs and in the final reaction to glycerol and a total of three FFAs. ATGL, adipose triglyceride hydrolase; HSL, hormone-sensitive lipase; MGL, monoglyceride lipase; CGI-58, comparative gene identification-58; G0S2, G0/G1 switch gene 2; TG, triglyceride; DG diacylglycerol; MG, monoacylglycerol; G; glycerol

### 1.2.1. ATGL

In 2004, three groups independently discovered an enzyme with TG hydrolase activity. This novel TG hydrolase with cytosolic acyl-hydrolase activity in white AT was named ATGL, desnutrin or phospholipase A2 $\zeta$  (Zimmermann et al. 2004, Jenkins et al. 2004, Villena et al. 2004). Now the enzyme is formally annotated as patatin-like phospholipase domain-containing protein 2 (PNPLA2) (Wilson et al. 2006). ATGL is highly expressed in AT and its expression significantly increases during adipogenesis (Villena et al. 2004). In addition, ATGL expression is also observed in cardiac and skeletal muscle, liver and other tissues (Haemmerle et al. 2006, Jocken et al. 2008, Reid et al. 2008).

Murine ATGL is a 468 amino acid protein with a molecular weight of 54 kDa, involved in the mobilization of TG stores (Zechner et al. 2009). The human gene encodes for a 504 amino acids protein with a molecular mass of 56 kDa (Zimmermann et al. 2004). Human and murine ATGL share a 84% sequence identity of the primary structure and >95% identity within the patatin domain, harbouring the active site of the enzyme. This structural motif has an unusual topology that differs from classical lipases and is responsible for its lipid hydrolase activity (Zechner et al. 2009). In comparison to other TG hydrolases, the active site of ATGL is not composed of a catalytic triad. Instead, the enzymatic activity of the patatin domain depends on a catalytic diad (Rydel et al. 2003).

Although the structure of ATGL is not yet known, mutational studies on human and murine ATGL revealed that the N-terminal part of the enzyme contains the catalytic patatin domain, while the C-terminal part, responsible for the regulation of the enzymatic activity, mediates the interaction with LDs (Duncan et al. 2010 Kobayashi et al. 2008, Schweiger et al. 2008).

ATGL is a specific TG hydrolase and also exhibits activity towards other lipid substrates like DGs, MGs, retinylesters (RE), or cholesterylesters (CE). However, ATGL has a 10-fold higher substrate specificity for TG than DG and therefore efficiently catalyzes the first step in TG hydrolysis (Zimmermann et al. 2004). Besides these functions *Notari et al.* suggested, that ATGL has a potent phospholipase A<sub>2</sub> activity, liberating FAs from eukaryotic membranes (Notari et al. 2006).

Overexpression of ATGL in murine adipocytes causes a stimulation of basal and catecholamine-induced lipolysis, whereas knockdown of ATGL results in a decrease of glycerol and free FA release (Kershaw et al. 2013). ATGL deficiency in mice leads to significant TG accumulation in white fat cells, which is associated with a decrease in FFA release (Haemmerle et al. 2006). ATGLs activity is potently inhibited by a small protein termed G0/G1 switch gene 2 (G0S2) (Yang et al. 2010). The full lipolytic activity of ATGL is dependent on the interaction of the patatin domain with the co-activator protein CGI-58. For this reason a direct protein-protein interaction between ATGL and CGI-58 is necessary for the development of the full enzymatic activity (Schweiger et al. 2008, Granneman et al. 2007, Cornaciu et al. 2011).

### **1.2.2. CGI-58**

As mentioned in the previous section, TG hydrolase activity of ATGL is strongly stimulated by the addition of CGI-58, also known as  $\alpha/\beta$  hydrolase domain containing protein 5 (ABHD5) (Lass et al. 2006). CGI-58 has a molecular weight of 39 kDa and belongs to the esterase/ thioesterase/ lipase superfamily of proteins, which are characterized by the presence of  $\alpha/\beta$  hydrolase folds.

In contrast to most other members of the protein family, the nucleophilic serine within the canonical esterase/lipase motif is replaced by an asparagine in CGI-58, effectively eliminating the possibility to function as a lipase.

In addition to ATGL binding, CGI-58 is also located at LDs through the interaction with Perilipin 1 (PLIN1) (Subramanian et al. 2004, Vallet-Erdtmann et al. 2004, Yamaguchi et al. 2004). Upon stimulation of lipolysis, PLIN1 gets phosphorylated by protein kinase A (PKA), which leads to the dissociation of PLIN1-bound CGI-58. Subsequently, CGI-58 interacts and activates ATGL (Granneman et al. 2009).

Addition of CGI-58 to murine ATGL causes a 20-fold increase in TG hydrolase activity. Human CGI-58 also has the potential to stimulate the enzymatic activity of ATGL, although the magnitude of activation is less pronounced (~5-fold) (Lass et al. 2006). Until now the molecular mechanism of ATGL activation by CGI-58 is still unclear. But it is possible that the interaction between ATGL and CGI-58 leads to conformational changes, substrate presentation, or removal of inhibitory reaction products. Besides its regulatory function in lipolysis, human and mouse CGI-58 also exhibit CoA-dependent lysophosphatidic acid acyltransferase (LPAAT) activity (Ghosh et al. 2008, Gruber et al. 2010, Montero-Moran et al. 2010).

The discovery of ATGLs co-activator CGI-58 was of great importance, because this finding provided a biochemical explanation for a rare human disorder. Mutations in the gene coding CGI-58, lead to a lipid storage disorder designated as "neutral lipid storage disease" (NLSD) or Chanarin Dorfman Syndrome (Lefèvre et al. 2001). NLSD is a rare, autosomal genetic disorder characterized by systemic TG accumulation in all tissues of the body, which leads to variable forms of skeletal and cardiac myopathy and hepatic steatosis (Chanarin et al. 1975). Besides mutations in CGI-58 also numerous mutations in the gene for ATGL were reported to cause NLSD (Schweiger et al. 2009).

### **1.3. Hormonal regulation of lipolysis**

In the last years, the existence of a physiological system that maintains energy homeostasis in response to variable access to nutrition and energy demand became evident. To preserve this balance, the system integrates afferent signals converging within the hypothalamus, which includes onset or termination of meals and long-term status of body energy stores. After the integration of these signals, direction and magnitude of efferent responses are determined, regulating the intensity of hunger, the level of energy expenditure and the levels of key circulating hormones such as adrenalin and insulin (Flier et al. 2004). These lipolytic and anti-lipolytic effectors control the catabolism and anabolism of stored fat in various tissues (Langin 2006a). The adrenal medullary catecholamines adrenaline and noradrenaline, both released from sympathetic nerve fibers, are the main initiators of lipolysis, whereas pancreatic insulin is a potent inhibitor (Froesch et al. 1965, Prigge and Grande 1971).

#### **1.3.1. Catecholamines**

The most potent stimulatory signals of lipolysis in the AT are catecholamines (adrenaline, noradrenaline), which act on  $\beta$ -adrenergic receptors ( $\beta$ -ARs) on the cell surface of adipocytes (Lafontan & Berlan 1993). Murine fat cells express three different subtypes of  $\beta$ -ARs, which includes  $\beta_1$ -AR,  $\beta_2$ -AR and  $\beta_3$ -AR. In human adipocytes only  $\beta_1$  and  $\beta_2$  receptors are capable of stimulating lipolysis (Holm 2003, Collins et al. 2004). In addition to their stimulatory functions, catecholamines also exhibit inhibitory effects on lipolysis, depending on their relative affinity for different ARs. For the activation of lipolysis  $\beta$ -ARs need to be activated, whereas  $\alpha_2$ -ARs are responsible for transmitting anti-lipolytic signals (Robidoux et al. 2004). Both AR types belong to the G-protein-coupled receptor (GPCR) family. And while  $\alpha_2$ -ARs are associated with the inhibitory  $G_i$  subunit, G-proteins of  $\beta$ -ARs contain the stimulatory  $G_s$  subunit (Lafontan & Berlan 1993).

Upon activation of the sympathetic nervous system, noradrenaline is released from the nerve fibers into AT and binds to  $\beta$ -ARs, which leads to the stimulation of adenylate cyclase (AC) through the stimulatory  $G_s$  subunit of the GPCR (Robidoux et al. 2004). The activation of AC initiates the conversion of adenosine triphosphate (ATP) to cyclic adenosine monophosphate (cAMP), resulting in an

intracellular increase of cAMP levels, which leads to the activation of PKA (Langin 2006). After activation, PKA phosphorylates the LD-associated protein PLIN1 and the cytoplasmic lipase HSL (Greenberg et al. 1991, Strålfors et al. 1984). Phosphorylation of PLIN1 subsequently leads to the release of PLIN1-bound CGI-58 (Lass et al. 2006, Granneman et al. 2009). The release of CGI-58 enables the interaction and subsequent activation of ATGL, initiating the lipolytic cascade (see Figure 2).

In addition, the phosphorylation of HSL causes an activation and translocation of the lipase from the cytosol to the LD surface (Egan et al. 1992). After the binding to phosphorylated PLIN1, HSL is activated and gains access to its DG substrate, which is generated by the TG hydrolase activity of ATGL (Shen et al. 2009, Wang et al. 2009).

### **1.3.2. Insulin**

The most potent inhibitory hormones of lipolysis are represented by insulin and insulin-like growth factor (IGF). In this inhibitory process, antagonization of catecholamine-induced lipolysis through the activation of phosphodiesterase 3B (PDE3B) is the main mechanism of insulin action. The activation of PDE3B leads to the degradation of intracellular cAMP, associated with decreased PKA activity. The decline of the enzymatic activity of PKA results in reduced phosphorylation of HSL and PLIN1, which leads to reduced TG hydrolysis. Binding of insulin to the insulin receptor (IR) activates the intrinsic tyrosine kinase and induces the phosphorylation of insulin receptor substrate (IRS) protein (Degerman et al. 1998). The phosphorylation of tyrosine residues of IRS creates recognition sites for effector proteins containing Src homology 2 (SH2) domains, like phosphatidylinositol 3-kinase (PI3K) (Tamemoto et al. 1994).

PI3K then activates the serine/threonine protein kinase B (Akt), which is required for the insulin-induced activation of PDE3B and the anti-lipolytic action of insulin (Kohn et al. 1996, Berggreen et al. 2009).

In addition, insulin also inhibits lipolysis at the transcriptional level through down-regulation of ATGL. The effect of insulin on ATGL expression is also mediated by the PI3K/Akt signalling cascade. Activation of Akt upon binding of insulin to the

insulin receptor, leads to the phosphorylation and inactivation of the FoxO1 transcription factor. FoxO1 is a central regulator of metabolism, promoting the expression of ATGL through direct binding to the promoter region (Chakrabarti & Kandror 2009, Chakrabarti et al. 2011).

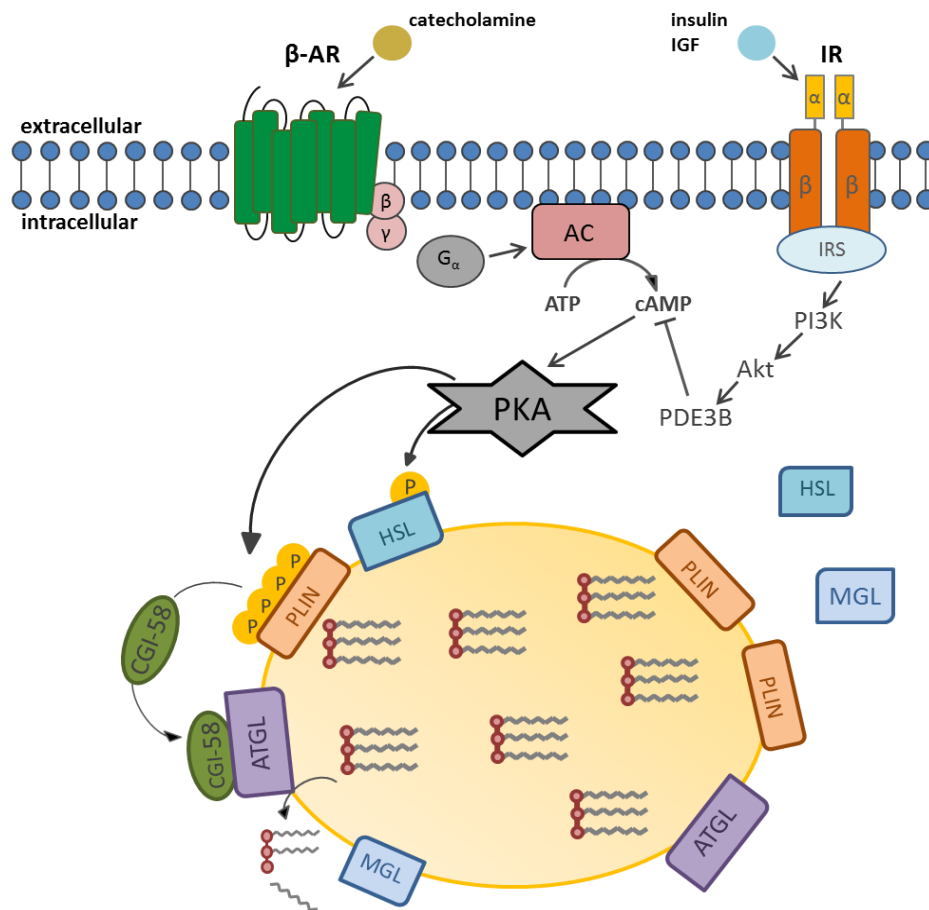


**Figure 2: Regulation of lipolysis.** Binding of pro-lipolytic hormones to  $\beta$ -adrenergic receptors ( $\beta$ -ARs) leads to the activation of AC through the  $\alpha$ -subunit of the heterotrimeric G-protein. Increased levels of cAMP activate PKA and the subsequent phosphorylation of HSL and PLIN. These phosphorylation events are necessary for enhanced lipolysis. Binding of the major anti-lipolytic hormone insulin to the IR causes the activation of PI3K. The kinase activity of PI3K activates Akt, which in turn activates PDE3B. The enzymatic activity of PDE3B lowers intracellular cAMP levels and inactivates PKA, associated with decreased lipolysis.

## 1.4. PEDF

Pigment epithelium-derived factor (PEDF) is a 50 kDa glycoprotein encoded by the *SERPINF1* gene (Carrell et al. 1987, Borg et al. 2011). PEDF consists of 418 amino acids. The N-terminal part contains a secretion signal peptide (1-19), a N-glycosylation site (Asn 285) and a serpin signature sequence (Becerra 2006, Steele et al. 1993). PEDF is expressed in most cell types and the mature gene product is secreted as a monomeric soluble glycoprotein starting at amino acid position 20 (Ortego et al. 1996, Petersen et al. 2003). In 1989, PEDF was first discovered by an American group led by L.V. Johnson. Experiments with conditioned media of human foetal retinal pigment epithelium cells revealed a pro-differentiating effect on Y-79 retinoblastoma cells (Tombran-Tink & Johnson 1989). Later a factor, responsible for neuronal differentiation, was isolated from the media and identified as PEDF (Becerra 1997). Analysis of the primary and three dimensional structure showed, that PEDF belongs to the serine protease inhibitor (SERPIN) superfamily (Carrell et al. 1987). Although PEDF has a typical protein fold for serine protease inhibitors, it does not inhibit these enzymes (Filleur et al. 2009). The reason for this missing function possibly lies in the structural characteristics of the exposed reactive loop (Huber & Carrell 1989). In comparison to typical SERPINS, the cleavage at this loop does not induce the typical stress-to-relax conformational change (Notari et al. 2006). For this reason PEDF has no demonstrable serine protease inhibitory activity and belongs to the non-inhibitory serpins (Becerra et al. 1995). It is feasible that this "defect" enabled PEDF to acquire additional properties, indicated by its multiple functions (see Figure 3).

About a decade after its discovery as a pro-differentiating and survival factor for neuronal cells, PEDF was identified as a potent endogenous inhibitor of angiogenesis in the eye (Tombran-Tink & Barnstable 2003, Dawson 1999). Evidence accumulated that PEDF also plays an important role as anti-angiogenic factor in solid tumors. In addition, PEDF exhibits anti-proliferation, anti-migration, pro-differentiation and pro-apoptosis effects on several cancer types (Fernández-Barral et al. 2014). The anti-angiogenic and anti-metastatic effect of PEDF mainly bases on antagonizing the vascular endothelial growth factor (VEGF) (Dawson 1999).

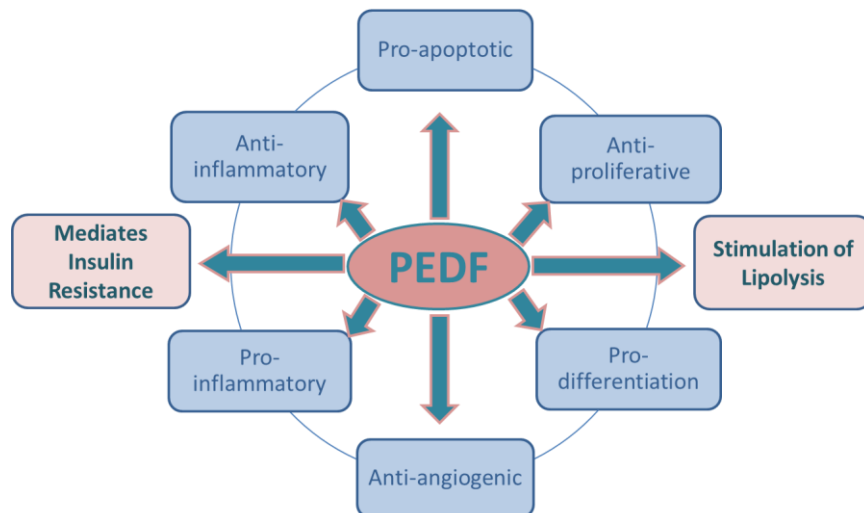


**Figure 3: The multiple roles of PEDF.** PEDF shows direct anti-tumor effects through its pro-apoptotic, anti-proliferative and pro-differentiation effects as well as indirect anti-tumor properties through pro-inflammatory, anti-angiogenic properties. Besides these functions PEDF also exhibits a stimulatory effect on lipolysis and seems to be involved in the development of insulin resistance.

In the last decade the research community paid more and more attention to PEDFs role as a novel adipokine involved in lipid metabolism. Recent studies revealed that PEDF expression levels in AT positively correlate with obesity and insulin resistance (Crowe et al. 2009). Clinical studies also confirmed that plasma PEDF is elevated in obese patients with metabolic syndrome and type 2 diabetes (Wang et al. 2008, Yamagishi et al. 2006, Joham et al. 2012). *Borg et al. (2011)* showed that PEDF increased basal lipolysis by 25% in isolated AT, whereas  $\beta$ -adrenergic stimulation was not further increased by the addition of PEDF. In experiments with explants from ATGL knockout mice the stimulatory effect of PEDF was not evident, indicating that PEDFs effect on lipolysis is ATGL-dependent. Additionally, plasma PEDF levels increased during fasting conditions and decreased after refeeding, consistent with rates of lipolysis. These results also support the putative pro-lipolytic role of PEDF.

The pro-lipolytic effect of PEDF could also represent the link to insulin resistance. It is well known that obesity is characterized by increased basal lipolysis and elevated circulating levels of FFAs, leading to ectopic lipid deposition and insulin resistance (Wolfe 1987). Since PEDF is known to acutely increase lipolysis in cultured 3T3-L1 cells *ex vivo* and in mice *in vivo*, it is possible that PEDF contributes to the desensibilization of circulating insulin (Crowe et al. 2009). In

addition, PEDF is involved in inflammatory signalling in several cell types and circulating PEDF levels correlate with the inflammatory state in patients with type 1 diabetes (Filleur et al. 2009, Jenkins et al. 2007). This is consistent with the finding that PEDF directly activates several inflammatory signalling proteins in skeletal muscle and liver, associated with reduced insulin signal transduction (Crowe et al. 2009).

The mechanism how PEDF exerts its pro-lipolytic action is mainly unknown and needs to be elucidated. However, it is likely that PEDFs action depends on a ligand-receptor mechanism, because its effects are blocked by antibodies, which act as cell surface-binding antagonists (Notari et al. 2006). *Notari et al.* recently proposed ATGL as a putative receptor for PEDF, inserted in the cell membrane with potent phospholipase A<sub>2</sub> activity.

#### **1.4.1. PEDF and ATGL**

In the last years researchers managed to identify a gene, encoding for a PEDF receptor (PEDF-R), by means of a two-hybrid system. A closer look at the cDNA sequence revealed a mRNA transcript of 2122 base pairs, coding for a protein with a molecular mass of 55,3 kDa. Further analysis showed that this receptor shares a strong homology with members of the PNPLA2-calcium-independent PLA<sub>2</sub> (iPLA<sub>2</sub>)/nutrin family and is identical to ATGL. Members of the PNPLA<sub>2</sub> protein family exhibit strong TG lipase, acylglycerol transacylase as well as phospholipase activities (Notari et al. 2006).

Due to the high level of sequence homology between ATGL and PNPLA3 (adiponutrin), *Notari et al. (2006)* hypothesized that ATGL is inserted into the cell membrane and acts as a receptor for PEDF. Additionally, hydrophobicity plots also predicted this transmembrane nature for ATGL, with four transmembrane domains interrupted by two extracellular loops and 3 intracellular regions (see Figure 4).

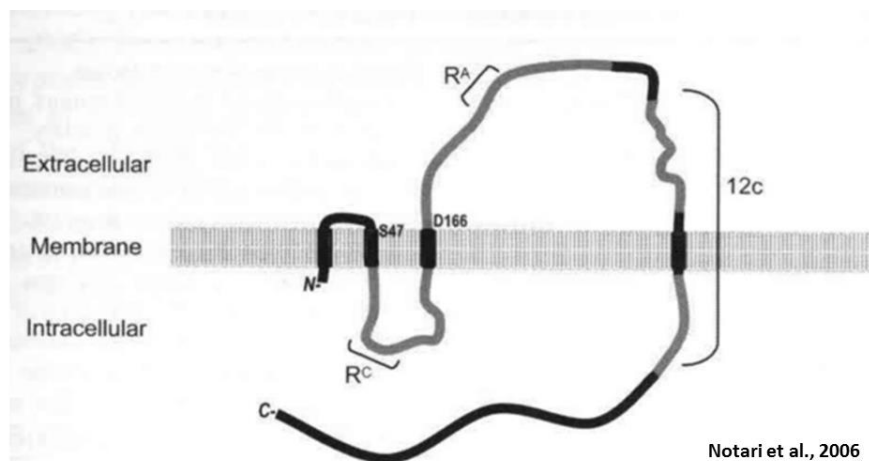


**Figure 4: Predicted transmembrane structure of ATGL.** Based on *in silico* information and the primary protein structure, a transmembrane nature for ATGL was predicted. In this model ATGL has four transmembrane domains with two extracellular loops and three intracellular regions and shows phospholipase activity upon binding to PEDF.

Sequence alignments of ATGL revealed a patatin phospholipase-like region with a Ser/Asp dyad, which resembles with the active sites in the catalytic domains of human cytosolic phospholipases. A<sub>2</sub> (cPLA<sub>2</sub>) (Hirschberg et al. 2001).

Phospholipase activity assays revealed an optimal enzymatic activity of ATGL at pH 7,5 in the presence of 0,1% Nonidet (NP) P-40. This activity was further stimulated by the addition of increasing amounts of PEDF, indicating that PEDF specifically stimulates the PLA enzymatic activity of ATGL *in vitro*. The phospholipase A<sub>2</sub> activity of ATGL is of special interest, because the released lipids serve as second messengers or precursors for eicosanoids, which are involved in signal transduction events. This suggests that PEDFs action is exerted via a lipid signalling pathway mediated by ATGL. It is suggested, that plasma membrane-associated ATGL produces extracellular bioactive lipids upon binding of PEDF, which can diffuse back into the cell and serve as signalling molecules (Notari et al. 2006).

A recent study also proposed a novel intracellular function of PEDF in regulating TG degradation. *Dai et al. (2013)* showed that PEDF facilitates the translocation of ATGL to LDs. This suggests that decreased levels of hepatic PEDF may contribute to hepatic steatosis phenotype in obesity.

Furthermore, their results indicated that PEDFs intracellular effect on TG degradation is dependent on the direct interaction with the C-terminal part of

ATGL. Long-term PEDF administration in mice caused a significant down-regulation of G0S2 expression in liver, whereas knockdown of PEDF in hepatocytes promotes G0S2 expression. Although this results suggest that PEDF promotes TG hydrolase activity through down-regulation of the inhibitory protein G0S2, further experiment need to be conducted to elucidate the exact mechanism of PEDFs action (Dai, Zhou, et al. 2013).

### **1.5. Aim of this thesis**

PEDF has been shown to affect lipid metabolism. However so far, contradictive results have been published on the possible mechanism of PEDFs pro-lipolytic function.

Hence the aim of my study was to investigate the effect of PEDF on adipocytes lipolysis. For this purpose I peromed TG hydrolase as well as PLA activity assays with ATGL in the presence and absence of PEDF.

To elucidate PEDFs pro-lipolytic effect on cultured adipocytes *ex vivo*, 3T3-L1 cells were transduced with a lentiviral construct for stable integration and inducible expression of PEDF. The release of FFAs and glycerol was measured in the presence and absence of PEDF. Additionally, western blot analysis was performed with 3T3-L1 cells to analyze the expression levels of key lipolytic enzymes. Since PEDF is secreted and believed to exert its stimulatory effect by a ligand-receptor mechanism, I decided to incubate 3T3-L1 cells with PEDF containing medium.

Although it is known that PEDF interacts with ATGL, I decided to perform Co-immunoprecipitation to verify ATGL-PEDF interaction and to identify new potential interaction partners involved in the lipolytic process.

## 2. Materials

---

## 2.1. Media

LB medium	10 g/l peptone 10 g/l NaCl 5 g/l yeast extract
SOC medium	5 g/l Yeast Extract 20 g/l tryptone 10 mM NaCl 2,5 mM KCl 10 mM MgCl <sub>2</sub> 10 mM Mg SO <sub>4</sub> 20 mM glucose
LB agar plates	10 g/l peptone 10 g/l NaCl 5 g/l yeast extract 15 g/l agar
Dulbecco's modified Eagle's medium high glucose (4,5 g/l) (DMEM) +/+	commercially available Gibco by Life Technologies 10% fetal calf serum 100 U/ml penicillin; 100 µg/ml streptomycin
Freeze medium	4 ml DMSO 6 ml fetal calf serum 10 ml DMEM (+/+)

0,25% Trypsin- EDTA

commercially available  
Gibco by Life Technologies

Fetal calf serum (FCS)

commercially available  
Gibco by Life Technologies

## 2.2. Buffers and Solutions

0,1 M  $KPO_4$  buffer (pH 7,2)

283  $\mu$ l 1M  $K_2HPO_4$   
717  $\mu$ l 1M  $KH_2PO_4$   
dilute to 10 ml with ddH<sub>2</sub>O

RIPA buffer (pH 7,5)

50 mM Tris/HCl  
150 mM NaCl  
1 mM EDTA  
1% NP-40  
1 mM PMSF

HSL buffer (pH 7)

0,25 M sucrose  
1 mM EDTA  
1 mM DTT  
1 x Pi  
(Antipain/ Leupeptin/ Pepstatin)  
2  $\mu$ g/ml 20  $\mu$ g/ml 1 $\mu$ g/ml

1 x PBS (pH 7,3)

140 mM NaCl  
2,7 mM KCl  
10 mM  $Na_2HPO_4$   
1,8 mM  $KH_2PO_4$

4 mM Oleic acid complexed to BSA	24,3 mg 8 mM oleic acid/ 10ml 1 x PBS 1,62 g 2,7 mM FFA free BSA/ 10 ml 1 x PBS heat to 37 °C add BSA solution drop wise to oleic acid (1:1)
----------------------------------	---

### **SDS-Polyacrylamid gelectrophoresis**

10 x Tris-Glycin buffer	200 mM Tris 1,6 M Glycin 0,83% SDS
4 x Lower buffer (pH 8,8)	0,5 M Tris 0,4% SDS stored at 4 °C
4 x Upper buffer (pH 6,8)	0,5 M Tris stored at 4 °C
4 x SDS loading buffer	0,2 M Tris 10% $\beta$ -mercaptoethanol 8% SDS 40% glycerin bromphenol blue (tip of a spatula)

### **Western Blot**

CAPS transfer buffer (pH 11)	10 mM CAPS 10% methanol
------------------------------	----------------------------

1 x TST (pH 7,4)	50 mM Tris/HCl 0,15 M NaCl 0,1% Tween 20
Coomassie staining solution	50% ethanol 7,5% from 80% acetic acid 0,25% coomassie-brilliant blue R250
Coomassie destaining solution	10% from 80% acetic acid 30% methanol
Stripping buffer (pH 6,7)	62,5 mM Tris 2 % SDS ad
<b><u>Agarose gelelectrophoresis</u></b>	
Agarose 1,5%	294 ml ddH <sub>2</sub> O 4,5 g agarose 6 ml 50 x TAE
1 x TAE buffer (pH 7,2)	40 mM Tris/HCl 50 mM EDTA 7% glacial acetic acid
5 x DNA loading dye	9 % glycerol 2,5 mg/ml bromphenol blue 2,5 mg/ml xylen- cyanol

### **Antibiotics**

Ampicillin sodium salt	Carl Roth GmbH
Doxycycline hyclate	Sigma-Aldrich, St. Louis
Puromycin	Sigma-Aldrich, St. Louis
Geneticin (G418 sulfate)	Life Technologies

### **Enzymes and Buffers**

Restrictions enzymes	New England BioLabs Inc.
10 x NEB Cutsmart buffer	New England BioLabs Inc.
Phusion High-Fidelity Polymerase	Finnzymes
10 x Phusion GC reaction buffer	Finnzymes
NEB T4 DNA Ligase	New England BioLabs Inc.
NEB T4 Ligase reaction buffer	New England BioLabs Inc.

### **Resins and Beads**

ANTI-FLAG® M2 Affinity Gel	Sigma-Aldrich, St. Louis
TALON® Metal Affinity Resins	Clontech Laboratories, Inc.

### **Differentiation 3T3-L1**

Forskolin	Sigma-Aldrich, St. Louis
IBMX	Sigma-Aldrich, St. Louis
Dexamethasone	Sigma-Aldrich, St. Louis

### 2.3. Primers

The primers used for cloning are listed below including their sequence and specificity for restriction enzymes. The sequences contain the complete open reading frame of PEDF. All oligonucleotides were purchased from Eurofins Genomics and diluted to a final concentration of 100 pmol/ $\mu$ l.

**Table 1:** Oligonucleotides used for cloning

<b>Primer</b>	<b>Sequence</b>	<b>Specificity</b>	<b>Tm (°C)</b>
N-His-PEDF_fw.	AAA GGT ACC ACA GGC CCT GGT GCT ACT CCT C	<i>KpnI</i>	72,2
N-His-PEDF_rev.	TGG CGG CCG CTT AAG TAC TAC TGG GGT CCA GGA TTC TGC	<i>NotI</i>	>75
C-Flag-PEDF_fw.	CTT GCG GCC GCG ATG CAG GCC CTG GTG CTA CTC	<i>NotI</i>	>75
C-Flag-PEDF_rev.	TCG GTA CCA GAG TGC TAC TGG GGT CCA GGA TTC T	<i>KpnI</i>	73,1
Lenti-PEDF_fw.	CTT GCG GCC GCG ATG CAG GCC CTG GTG CTA CTC	<i>NotI</i>	> 75
Lenti-PEDF_rev.	CTA GAA TTC TTA AGT GCT ACT GGG GTC CAG GAT TCT G	<i>EcoRI</i>	70,6

## 2.4. Vectors

pcDNA4/HisMaxC vector (Invitrogen Life Technologies, San Diego, USA) was used for the introduction of a polyhistidine-tag (6 x His) on the N-terminus of PEDF. This vector is designed for the overexpression of recombinant proteins in mammalian cell lines. To achieve high-level expression of the protein of interest, the vector is equipped with a CMV promoter and a translational QBI SP163 enhancer sequence. As a selection marker a zeocin resistance gene is provided, which is under the control of a SV40 promoter. Recombinant proteins containing a N-terminal His-tag were expressed in COS-7 cells, for triglyceride and phospholipase assays and for Co-immunoprecipitation studies.

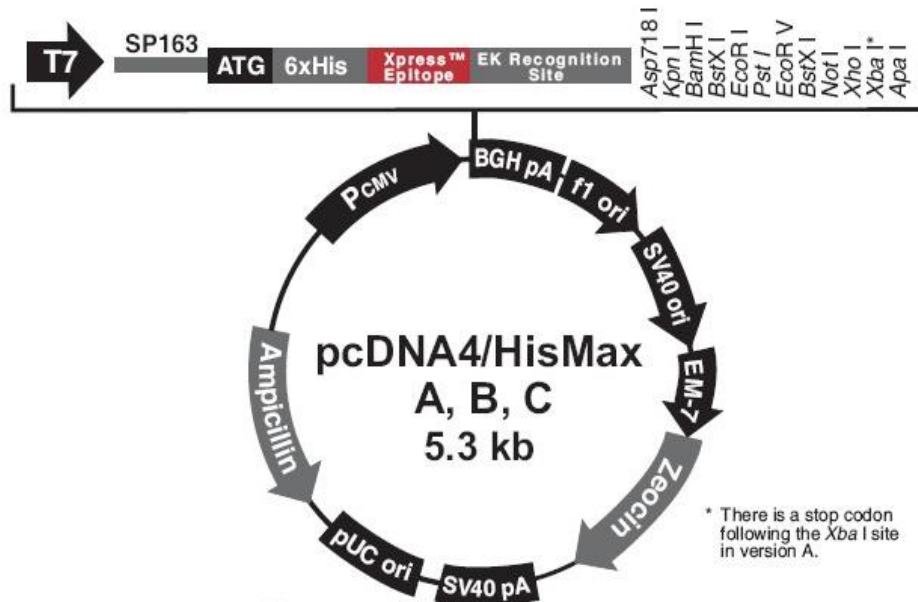


**Figure 5: pcDNA4/HisMacX expression vector.** Expression of the gene of interest is regulated from a CMV promoter. Furthermore, the vector contains a polyhistidine (6 x His) sequence upstream of the multiple cloning site for the introduction of a His-tag to the N-terminal region of recombinant protein.

pFLAG-CMV-5.1 vector (Sigma-Aldrich, St. Louis, USA) was used for the introduction of a Flag octapeptide (DYKDDDDK) on the C-terminus of PEDF. The Flag-tag is located downstream of the multiple cloning site, which enables a C-terminal linking to the protein of interest. The CMV promoter region drives the transcription of the Flag-fusion construct in various mammalian cell lines. The multiple cloning region of the vector is not preceded by a translational initiation

signal. Therefore a translational start signal must be included into the coding sequence during primer design. Additionally, the vector contains an ampicillin resistance gene.

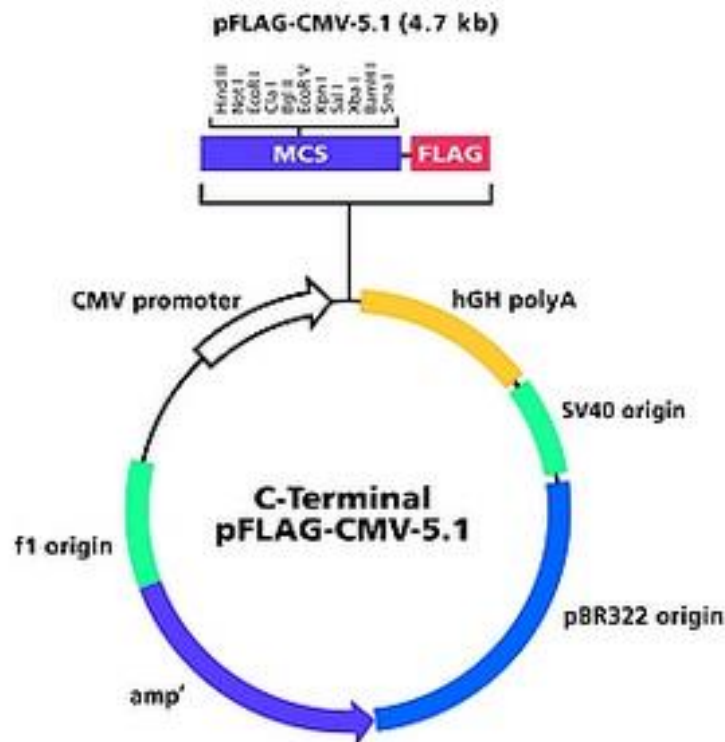


**Figure 6:** The pFLAG-CMV-5.1 expression plasmid. The expression of the gene of interest is under control of the CMV promoter. The sequence for the Flag tag is located downstream of the multiple cloning site.

pLVX-Tight-Puro (Clontech Laboratories, Inc.) is a tetracycline (Tet)-inducible, lentiviral expression vector. This vector is designed for an inducible expression of a gene of interest under the control of  $P_{Tight}$ , a modified Tet-responsive promoter. The promoter contains a modified part of the CMV promoter, and seven direct repeats of a 36 bp regulatory sequence including the 19 bp tet-operator sequence. This vector was used for the transfection of HEK-293 packaging cells and transduction of 3T3-L1 cells for stable PEDF integration into the genome. For the integration of genetic material into the host genome, the vector is equipped with 5'- and 3'-LTRs (long terminal repeats). In addition, the vector contains an ampicillin resistance gene for the selection of positive clones. The expression of

PEDF was induced through withdrawal of Doxycycline, which allows the binding of the tet-transactivator protein within the promoter region.

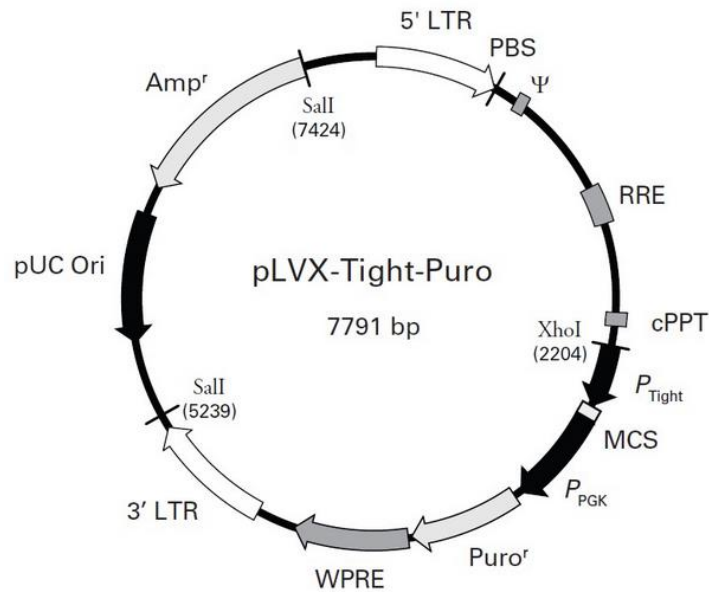


**Figure 7: The pLVX-Tight-Puro expression plasmid.** The expression of the gene of interest is under the control of the  $P_{Tight}$  promoter, which allows a tightly regulated, Doxycycline-mediated expression. In order to function, the system requires the co-expression of a tetracycline-controlled transcriptional activator encoded from the packaging mix vectors.

## 2.5. Bacterial strains

### *E. coli* DH5 $\alpha$

This chemically competent *E.coli* strain is often used for cloning procedures, because of its high transformation efficiency. *E.coli* cells were obtained from New England BioLabs Inc. (Germany). Genotype: *fhuA2*  $\Delta$ (*argF-lacZ*)U169 *phoA* *glnV44*  $\Phi$ 80  $\Delta$ (*lacZ*)M15 *gyrA96* *recA1* *relA1* *endA1* *thi-1* *hsdR17*

## 2.6. Cell lines

### Cos-7

COS (an abbreviation for CV-1 in Origin with SV40 genes) cells are a laboratory cell line derived from the African Green Monkey, *Cercopithecus aethiopus* (Cos-7.com). The cells were obtained from the American Type Culture Collection (ATCC, Rockville, Maryland) and cultivated in Dulbecco's modified eagle medium

(DMEM) containing 4,5 g/ml glucose, 10% FCS and 1% penicillin/streptomycin at 37 °C in 7,5% CO<sub>2</sub>, 95% humidified atmosphere. This cell line was used for transfection and production of cell lysates.

### **HEK-293**

HEK-293 is a cell line derived from human embryonic kidney cells. This laboratory cell line was initiated by the transformation of HEK cells with sheared fragments of adenovirus type 5 DNA (HEK293.com). The cells were obtained from the American Type Culture Collection (ATCC; Rockville, Maryland) and cultured in Dulbecco's modified eagle medium (DMEM) containing 4,5 g/ml glucose, 10% FCS and 1% penicillin/streptomycin at 37 °C in 7,5% CO<sub>2</sub>, 95% humidified atmosphere. This cell line was used for transfection and production of cell lysates.

### **3T3-L1**

The preadipocyte cell line was originally developed by clonal expansion from murine Swiss 3T3 cells. The addition of pro-differentiative agents induces the conversion from the fibroblastic phenotype to adipocytes (Zebisch et al. 2012). Cells were obtained from the American Type Culture Collection (ATCC; Rockville, Maryland) and cultured in Dulbecco's modified eagle medium (DMEM) containing 4,5 g/ml glucose, 10% FCS and 1% penicillin/streptomycin at 37 °C in 7,5% CO<sub>2</sub>, 95% humidified atmosphere.

## 2.7. Antibodies

Table 2: Antibodies used for western blot analysis

Antibody	Source	Dilution
Anti-His N-terminal	Amersham Biosciences (Uppsala, Sweden)	1:5 000 in 1 x TST plus 5% milk
Anti-Flag-HRP	Sigma-Aldrich (St. Louis, USA)	1:5 000 in 1 x TST plus 5% milk
Anti-SerpinF1 (PEDF)	Sigma-Aldrich (St. Louis, USA)	1:2 000 in 1 x TST plus 5% milk
Anti-ATGL	Cell Signaling Technology Inc., Boston, MA	1:1 000 in 1 x TST plus 5% milk
Anti-phospho-HSL	Cell Signaling Technology Inc., Boston, MA	1:2 000 in 1 x TST plus 5% milk
Anti-HSL	Cell Signaling Technology Inc., Boston, MA	1:5 000 in 1 x TST plus 5% milk
SCD-1	Cell Signaling Technology Inc., Boston, MA	1:1 000 in 1 x TST plus 5% milk
Anti-phospho-PKA	Cell Signaling Technology Inc., Boston, MA	1:1 000 in 1 x TST plus 5% milk
Anti- $\alpha$ -Actin	Cell Signaling Technology Inc., Boston, MA	1:5 000 in 1 x TST plus 5% milk
Anti-Rabbit-HRP	Vector Laboratories, Inc. Burlingame	1:10 000 in 1 x TST plus 2% milk
Anti-Mouse-HRP	GE healthcare, UK Limited	1: 10 000 in 1 x TST plus 2% milk
Anti-Rabbit True-Blot	Rockland Inc.	1: 10 000 in 1 x TST plus 2% milk
Anti-Mouse True-Blot	Rockland Inc.	1: 10 000 in 1 x TST plus 2% milk

## 2.8. Kits

- **Pierce (Rockford, USA)**  
BCA (bicinchoninic acid) Protein Assay Kit
- **GE Healthcare (Chalfont St Giles, UK)**  
ECL Plus Western Blotting Detection System
- **Wako Chemicals GmbH (Neuss, Germany)**  
NEFA-HR(2) Wako R1a and NEFA-HR(2) Wako R1b reagents
- **Sigma-Aldrich (St. Louis, USA)**  
Free Glycerol Determination Kit
- **QUIAGEN N.V. (Venlo, The Netherlands)**  
NucleoBondXtra Plasmid Purification  
QIAprep Spin Miniprep Kit (250)  
PCR clean up Gel extraction  
NucleoBond® Xtra Midi / Maxi
- **NEB (Frankfurt am Main, Germany)**  
Q5 site-directed Mutagenesis Kit

# 3. Methods

---

### 3.1. Cloning

For specific functional protein studies, the protein has to be expressed in a cell line of interest. For this purpose, molecular cloning is the method of choice. The term molecular cloning refers to a process by which recombinant DNA molecules are produced and transformed into a host cell, where they are replicated (Neb.com 2014). Briefly summarized, the coding region of your gene of interest is amplified with PCR including restriction sites for the insertion into an expression vector. Afterwards the recombinant construct is transformed into the host cell for replication.

#### 3.1.1. Polymerase chain reaction (PCR)

To start with the cloning procedure a sufficient amount of your gene of interest (GOI) has to be generated. To amplify the target sequence, short complementary DNA stretches including the restriction sites for further cloning steps, need to be designed. In the course of this work, several PCRs were carried out with different primer mixes. All the PCRs were performed to amplify the complete coding sequence of PEDF with or without a specific tag. The optimal conditions for specific PEDF amplification are listed in Table 3 and 4.

Table 3: Standard PCR reaction for gene cloning.

<b>Components</b>	<b>Volume</b>
Template	1 $\mu$ l
Phusion HF DNA Polymerase	0,3 $\mu$ l
Buffer GC 5 x	5 $\mu$ l
Primer fw (0,5 $\mu$ M)	1 $\mu$ l
Primer rv (0,5 $\mu$ M)	1 $\mu$ l
dNTP mix (10mM)	1,6 $\mu$ l
DMSO (100%)	1 $\mu$ l
MgCl <sub>2</sub> (50 mM)	0,6 $\mu$ l
H <sub>2</sub> O	18, 5 $\mu$ l
<b>Total volume</b>	<b>30 <math>\mu</math>l</b>

Table 4: Program for standard PCR reaction.

	<b>Step</b>	<b>Temperature</b>	<b>Time</b>
	Initial denaturation	98 °C	30 sec.
<b>30 Cycles</b>	Denaturation	98 °C	20 sec.
	Annealing	59,2 °C	30 sec.
	Extension	72 °C	60 sec.
	Final extension	72 °C	5 min.

### 3.1.2. Gel electrophoresis

To confirm the amplification of the desired construct, PCR products were analyzed by agarose gel electrophoresis. Agarose gel electrophoresis is a method used to separate DNA according to size in an electric field. Negatively charged nucleic acids migrate towards the anode, where the migration flow is only determined by the size and conformation of the molecules. Therefore shorter molecules move faster and migrate farther through the pores of the gel than larger ones. The migration rate is also influenced by the conformation of the nucleic acid molecules. Supercoiled DNA moves faster than the relaxed or linear form, because it is more compact. To visualize the gel separated DNA molecules, ethidium bromide is added to the buffer as well as to the agarose gel. Ethidium bromide intercalates between the base pairs of the DNA and exhibits fluorescence upon UV-light exposure.

DNA samples were mixed with 5 x DNA loading dye and pipetted into slots of a 1.5% agarose gel, which contained ethidium bromide. Standard Gene Ruler™ 1 kb DNA Ladder (Thermo, Life Technologies) was used to analyze the size of the DNA fragments. The samples were separated in 1 x TAE buffer in an electrical field for 30 – 45 minutes at 90 V and 200 mA. Following separation the gel was photographed under UV-light using Master VDS (Pharmacia Biotech, Upsala Sweden). If the samples were needed for further cloning procedures the bands were cut out of the gel and purified using PCR clean up kit (see 2.8. Kits).

### **3.1.3. Restriction digest**

Restriction enzymes are endonucleolytic enzymes cutting double stranded DNA near or at a specific nucleotide sequence, known as recognition site. Through cleavage of the DNA backbone, either sticky or blunt ends are generated. Most restriction enzymes digest DNA asymmetrically across their recognition sequence, which results in a single stranded overhang on the digested end of the DNA fragment. These overhangs allow the vector and the insert to form bonds between complementary bases. The use of two different enzymes ensures the insertion of the insert in the right orientation and prevents the self-ligation of the digested vector.

The purified, in ddH<sub>2</sub>O solubilized insert DNA, as well as the plasmid DNA were digested at 37°C shaking at 350 rpm for 2 hours. The DNA samples (1 µg insert and 5 µg vector) were digested with 1 µl of each restriction enzymes (10 U/µl), in a buffer recommended by the supplier in a total volume of 60 µl.

### **3.1.4. Dephosphorylation of the vector**

To prevent re-ligation of the digested vector, newly generated 5'ends of the plasmid were dephosphorylated using calf intestine phosphatase (CIP). 1 µl CIP was added to the digested vector and incubated for 20 minutes at 37°C.

### **3.1.5. Phenol-Chloroform extraction**

To inactivate and remove the restriction enzymes from the digested DNA, an extraction with phenol and chloroform was performed. For this purpose the volume of the restriction mix was brought to a final volume of 100 µl with ddH<sub>2</sub>O. Afterwards an equal volume of phenol and 3/4 volume of chloroform was added. After thoroughly shaking, the mix was centrifuged at 8 000 rpm for 5 minutes at 4°C. The phenol phase (upper phase) was then removed carefully and transferred in a new reaction tube. For DNA precipitation 1 ml of cold ethanol (100%) was added to the reaction tube and incubated for 3 hours at -80°C. The incubation was followed by a 14 000 rpm centrifugation step for 30 minutes at 4°C for pelleting DNA. The DNA pellet was then washed with 70% ethanol and

dried at 37°C. DNA was then solubilized in 20 µl ddH<sub>2</sub>O, ready for the ligation step.

### **3.1.6. Ligation**

The final step of the cloning procedure is the connection of the GOI with the vector. This is achieved by the formation of covalent bonds between the sugar phosphate backbones of the two DNA fragments. Therefore the 3'-hydroxyl group of one fragment is covalently linked through the formation of a phosphodiester bond with the 5'-phosphate group of the other fragment. The optimal molar ratio of vector : insert for ligation is 1:3.

To estimate the concentration of the vector and insert DNA, 1 µl of each sample was separated on a 1,5% agarose gel. The ligation was performed with T4 DNA ligase at 20°C for 1 hour.

### **3.1.7. Transformation**

Transformation is defined as the process by which exogenous DNA is introduced into a bacterial cell. Therefore the cells must be in a competent state, achieved by the incubation with a solution containing cations or under cold conditions followed by a heat shock.

For the transformation an aliquot of chemically competent *E.coli* DH5α cells, stored at -80°C; was thawed on ice for 5 minutes. Then 25 µl of competent cells were incubated with 5 µl (about 50 ng) plasmid DNA. The tube was carefully flicked 4-5 times to mix cells and DNA. Afterwards the mixture was incubated on ice for 30 minutes. Subsequently, cells were then heat shocked by placing the tube into a 42°C water bath for 30 seconds. Following the heat shock cells were incubated on ice for 5 minutes. Transformed cells were resuspended in 250 µl pre-warmed SOC medium and grown in the shaking incubator for 1 hour at 37°C. Cells were plated on 10 cm LB plates containing 100 µg/ml ampicillin to identify the positive bacteria clones, which took up the recombinant plasmid. The LB plates were incubated over night at 37°C.

### **3.1.8. Small scale plasmid isolation - Miniprep**

Single colonies were picked and overnight culture (ONC) of 6 ml LB media, containing 100 µg/ml of ampicillin, was inoculated. ONCs were grown overnight at 37°C under constant shaking. Thereafter, cells were centrifuged at 5 000 g for 5 minutes. The recombinant plasmid DNA was then isolated according to the Miniprep Kit protocol (see 2.8. Kits). Finally, the DNA was eluted in 60 µl elution buffer.

### **3.1.9. Large scale plasmid isolation - Maxiprep**

To isolate a sufficient amount of plasmid, a Maxiprep was performed. Therefore 6 ml LB medium containing ampicillin was inoculated with a single colony and incubated at 37°C over day (ODC) under shaking. After 6-8 hours 250 µl of the ODC were transferred to 250 ml antibiotic containing LB medium and incubated at 37°C overnight with shaking. To isolate plasmids the Maxi Kit was used (see 2.8. Kits). The plasmid was dissolved in 100-200 µl ddH<sub>2</sub>O and the concentration was measured with Nano Drop.

### **3.1.10. Sequencing of the isolated DNA**

Isolated plasmid DNA was sequenced by Microsynth (Balgach, Switzerland) and sequence results were controlled using ClustalW2 alignment.

### 3.2. General information about lentivirus generation

To elucidate the intracellular effect of PEDF expression on lipolysis in differentiated 3T3-L1 cells, the lentiviral pLVX-Tight-puro Tet-off vector system was used (see Figure 8).

This system was chosen, because recombinant lentiviral vectors are powerful and efficient tools for the genomic integration of genetic material into various cell types (Ausubel et al., 1995, Coffin et al., 1996). The versatility of lentiviruses allows infection, transduction and sustained expression in almost any mammalian cell line, including dividing and non-dividing cells, stem cells, and primary cell cultures. In the first step the GOI is cloned into the pLVX-Tight-Puro vector, under the control of the tetracycline (Tet)-inducible  $P_{\text{Tight}}$  promoter. After finishing of the cloning procedure the lentiviral construct is transformed in *E.coli* DH5 $\alpha$  for amplification. Afterwards the recombinant pLVX-Tight-Puro construct containing the GOI is isolated from the selected positive clones and used for co-transfection of HEK-293 packaging cells together with the Lenti-X HTX Packaging Mix. The Lenti-X HTX Packaging Mix is a plasmid mixture that provides all the necessary lentiviral packaging components necessary for virus particle production in the packaging cell line (Wu et al., 2000). In a separate step, the pLVX-Tight-Puro construct is co-transfected with the pLVX-Tet-Off Advanced vector, which constitutively expresses the tetracycline-controlled transactivator, tTA-Advanced. The separate co-transfection in HEK-293 cells prevents the production of replication-competent lentiviruses, which enables a high safety standard. After assembly and transport of the viral cores to the cell membrane, infectious virus particles bud from the cell membrane of the HEK-293 packaging cells into the medium. The budding enables harvesting of infectious virions in the supernatant of the cultured cells without additional time consuming purification steps after 48 hours. To establish the complete Tet-Off System, 3T3-L1 target cells must be co-transduced with both virus particles containing supernatants.

The expression of PEDF is induced through removal of Doxycycline (tetracycline derivative), which allows the binding of the tetracycline-controlled transactivator in the  $P_{\text{Tight}}$  promoter region.

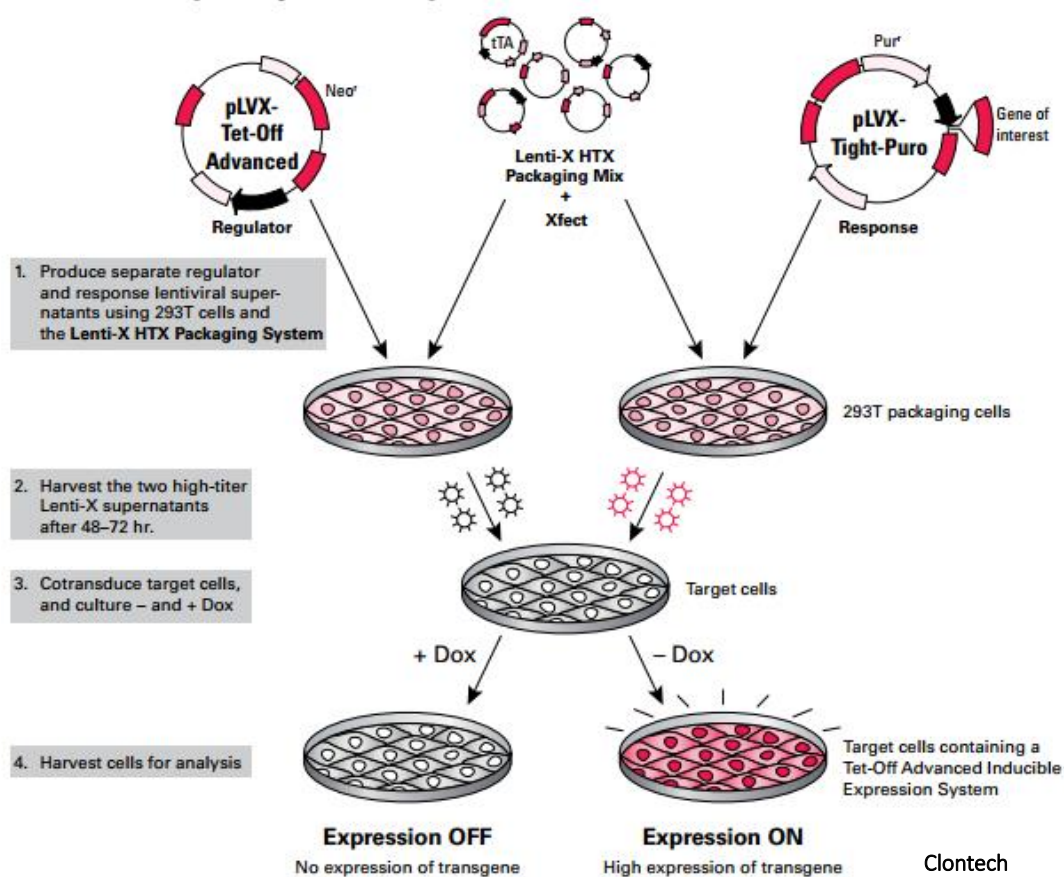


**Figure 8:** A schematic representation of the Tet-off Advanced system. For the generation of separate regulator and response lentiviral supernatants, HEK-293 cells were separately co-transfected either with pLVX-Tet-Off Advanced and Lenti-X HTX Packaging Mix or with pLVX-Tight-Puro containing the gene of interest and the Lenti-X HTX Packaging Mix. The Tet-Off Advanced system is inducible through withdrawal of Doxycycline from the medium.

### 3.2.1. Transfection of HEK-293 packaging cells

HEK-293 cells were used as packaging cells for the production of virus particles. For the transfection with the lentiviral construct and the packaging mix,  $6 \times 10^6$  cells were seeded in a 10-cm culture dish. The transfection procedure was conducted as usual (see 3.3.3. Transfection). Since the virus particles bud from the outer membrane of HEK-293 cells, the supernatant of cultured cells was collected after 48 hours and used for the following transduction.

### 3.2.2. Transduction of 3T3-L1 cells

For the transduction of 3T3-L1 preadipocytes with virus particles, cells were seeded in a 6-well plate. After addition of the supernatants, which contained the virus particles, cells were centrifuged at 1 200 g for 1 hour at 30°C. This

centrifugation step is important to bring the virus particles and 3T3-L1 cells in direct contact with each other. Before starting with the scale up, it is important to test the inducibility of the Tet-off system in 3T3-L1 cells by western blot analysis. After verification, 3T3-L1 cells were harvested and seeded in 12- well plates for differentiation (see 3.3.2. Differentiation of 3T3-L1 preadipocytes).

### **3.2.3. Selection and cultivation**

The successfully transduced 3T3-L1 cells were selected by the addition of puromycin (1,5 µg/ml) and genitacin (400 µg/ml). Prior the usage of these antibiotics for selecting transduced cells, optimal selection concentrations must be determined for 3T3-L1 cells. The toxic concentration of puromycin was 1,5 µg/ml and for genitacin 400 µg/ml. The working concentration of puromycin was 0,2 µg/ml and 50 µg/ml for genitacin.

### **3.2.4. Induction of the Tet-off system**

For a sufficient suppression of PEDF expression, 3T3-L1 cells were cultivated in the presence of 1µg/ml Doxycycline. PEDF expression was induced at the first day of differentiation through withdrawal of Doxycycline from the medium.

## **3.3. Cell culture**

### **3.3.1. Cultivation of cells**

Cells were cultivated in culture flasks (Greiner Bio-One GmbH, Frickenhausen, Germany) and stored in an incubator at 37°C, 5% CO<sub>2</sub> and 95% humidity. When the proposed confluence of each cell line (COS-7, HEK-293, 3T3-L1) was achieved, DMEM medium was removed from the flasks and cells were washed with 10 ml 1 x PBS buffer (see 2.2 Buffers and Solutions). 3 ml 0.05% Trypsin-EDTA solution (Gibco, Life Technologies) was added and cells were incubated in the incubator at 37°C until they were completely detached from the flask surface. To stop the trypsinization reaction, 10 ml medium containing FCS was added and the resulting cell suspension was transferred to a 50 ml tube and centrifuged for 3 minutes at 1 200 rpm. For sub-culturing purposes, the resuspended cells were splitted according to the manufactures splitting ratio.

It is important to note, that it is recommended that 3T3-L1 cells should never become confluent, otherwise they won't differentiate anymore.

Table 5: Seeding density of different cell lines.

	6-well plate	10-cm dish
<b>COS-7</b>	1,5 * 10 <sup>5</sup> cells	9 * 10 <sup>5</sup> cells
<b>HEK-293</b>		

### 3.3.2. Differentiation of 3T3-L1 preadipocytes

3T3-L1 preadipocytes were cultured in DMEM high glucose medium at 37°C, 5% CO<sub>2</sub> and 95% humidity. To start the differentiation procedure the cells have to be confluent. Two days after reaching confluency state, the differentiation process was started by changing the regular growth medium by DMEM high glucose containing 0,4 µg/ml dexamethasone, 20 µg/ml insulin, and 500 µM IBMX. To avoid precipitation of IBMX in the media it was heated at 60°C for 10 minutes. On the 3rd day of differentiation, the medium was replaced by DMEM high glucose containing 20 µg/ml insulin. On days 5 and 7 cells were cultured in DMEM high glucose supplemented with 0,4 µg/ml insulin. 3T3-L1 cells were fully differentiated to adipocytes at day 8. Experiments were performed one and two days after the cells were differentiated, respectively.

### 3.3.3. Transfection and preparation of cell lysates

Transfection is an often used non-viral method for introducing nucleic acids into eukaryotic cells. For the transfection of COS-7 and HEK-293 cells the polycationic transfection reagent Metafectene (Biontex GmbH, Munich, Germany) was used. It is important that the cells were in the exponential growth phase during DNA transfection, because the transfected DNA has to be transported into the nucleus during cell division for efficient expression.

COS-7 and HEK-293 cells were seeded at 900 000 cells/10-cm dish and cultivated in DMEM containing 10% FCS, 100 IU/ml penicillin and 100 µg/ml streptomycin. Cells were transfected with 6 µg DNA complexed to 18 µl Metafectene in DMEM medium without serum and antibiotics. After 4 hours the medium was replaced by regular growth medium. Twenty-four hours after

transfection, cells were washed three times with 1 x PBS, collected using a cell scraper and centrifuged at 1 200 rpm for 3 minutes. For the preparation of cell lysates, cells were disrupted in 300 µl HSL buffer by sonication at amplitude 1 for 10 seconds (Missonix Sonicator 4000, QSonica; Newtown, USA). Nuclei and unbroken cells were removed by centrifugation at 1 000 g, 4°C for 10 minutes. Protein concentration of cell lysates was determined using Bradford protein assay and BSA as standard. The expression of the recombinant proteins was verified by western blot analysis.

### **3.4. Measuring Protein content**

In the course of this work two different methods were used to measure protein concentration.

#### **3.4.1. BCA protein assay**

BCA protein assay is a copper-based protein assay for quantitation of protein concentration. BCA is compatible with samples that contain up to 5% detergents. Additionally it responds more uniformly to different proteins than Bradford and is 100 times more sensitive. The BCA Protein Assay combines the protein-induced biuret reaction with the highly sensitive and selective colorimetric detection of the resulting cuprous cation by BCA. There are two steps involved. First is the biuret reaction, where the reduction of cupric ion to cuprous ion leads to a colour change. The second step is the chelation of two BCA molecules with the cuprous ion, resulting in an intense purple color. The BCA/copper complex is water-soluble and exhibits a strong linear absorbance at 562 nm with increasing protein concentrations. Calibration curves are most commonly used to determine the concentration of proteins.

A BSA stock solution was used to generate a calibration curve (1 mg/ml; 0,5 mg/ml; 0,25 mg/ml; 0,125 mg/ml; 0,0625 mg/ml). For dilution of the BSA stock solution the same buffer was used as for diluting proteins. The protein concentration of each sample as well as the dilution points of the calibrations curve was measured as duplicates. Therefore 10 µl of the sample were pipetted into a microtiter plate, 200 µl BCA mix was added and incubated for 30 minutes

at 37°C. Afterwards the absorption was measured at 562 nm using Biotrak II Plate Reader (Amersham Biosciences, Cambridge, UK). To generate the standard curve, concentration was plotted on the X-axis, and absorption at 562 nm on the Y-axis. The calibration curve was calculated via Microsoft Excel®, which was then used to determine the protein concentration of the sample.

### **3.4.2. Bradford protein assay**

To determine protein concentrations in samples such as cell lysates, a Bradford protein assay was performed. The measurement is based on binding of Coomassie™ Brilliant Blue G-250 dye to basic amino acids in the acidic environment of the reagents. In the acidic environment of the reagent, proteins bind to the Coomassie dye. This results in a spectral shift of the dye from an absorbance maximum at 465 nm to an absorbance maximum at 610 nm. The Coomassie dye-protein complex is measured at 595 nm. The samples were diluted with the respective buffers.

A BSA stock solution was used to generate a calibration curve (0,4 mg/ml; 0,2 mg/ml; 0,1 mg/ml; 0,05 mg/ml, 0,025 mg/ml, 0,0125 mg/ml). All samples and standard dilutions were mixed with 200 µl 1:5 diluted Bio-Rad Protein Assay reagent. After a short incubation at room temperature, absorption at 595 nm was measured using a plate reader. Double determinations were done for each sample and the standard. To generate the standard curve, concentration was plotted on the X-axis, and absorption at 562 nm on the Y-axis. The calibration curve was calculated via Microsoft Excel®, which was then used to determine the protein concentration of the sample.

### **3.4.3. SDS-PAGE**

To analyze expression levels of proteins, samples were separated by discontinuous denaturing sodium dodecyl sulfate polyacrylamide gel electrophoresis (SDS-PAGE). Protein samples were mixed with 4x SDS loading buffer and heated for 10 minutes at 99°C. The samples were briefly centrifuged and loaded onto the gel. As a molecular weight standard, 5 µl of Precision Plus Protein All Blue Standard were loaded on the gel. Proteins were separated at 20

mA for approximately 90 minutes in 1x Tris-Glycin buffer (see 2.2 Buffers and Solutions) until the front reached the bottom. When SDS PAGE was finished the proteins were blotted onto a polyvenyldenfluorid (PVDF) membrane (Carl Roth GmbH, Karlsruhe, Germany).

### **3.5. Expression analysis**

#### **3.5.1. Western blot analysis**

Proteins were separated according to their molecular weight by SDS-PAGE (Sodium-dodecylsulfate-polyacrylamide gel electrophoresis) using a 10% polyacrylamide gel and 1x Tris-Glycine buffer. After gel electrophoresis proteins were transferred onto a polyvenyldenfluorid (PVDF) membrane in CAPS buffer at 200 mA for 1 hour. Thereafter the membrane was blocked with 10 % non-fat dry milk (Roth) dissolved in 1 x TST buffer. For detection of the proteins, the blots were incubated with different primary antibodies at different dilutions (see 2.7. Antibodies) in 1 x TST-buffer containing 5 % (w/v) non-fat dry milk and horseradish peroxidase-labeled secondary antibodies (see 2.7. Antibodies) at a dilution of 1:10,000 in 1 x TST containing 2 % (w/v) non-fat dry milk. Binding of the secondary antibody was visualized by enhanced chemoluminescence detection (Pierce ECL, Thermo Scientific).

### **3.6. Co-Immunoprecipitation**

Co-immunoprecipitation (Co-IP) is a widely used method to identify physiologically relevant protein-protein interactions. For this purpose, cell lysates were incubated with His- or Flag-tag specific antibodies covalently linked to agarose beads. After incubation the potential interaction partner of the tagged protein is co-immunoprecipitated by centrifugation.

For Co-IP, HEK-293 cell lysates containing overexpressed proteins of interest were used and incubated with Anti-Flag agarose beads (ANTI-FLAG® M2 Affinity Gel). For disruption of cell membranes, cells were incubated in 250 µl RIPA buffer containing 2% NP-40 for 30 minutes on ice. During this incubation period cells need to be resuspended several times to efficiently disrupt membranes. After

incubation, cells were further disrupted by shear force. For this purpose a 26 G syringe needle was used. This procedure needs to be repeated until cell suspension becomes turbid. Afterwards the cell suspension was centrifuged at 1 000 g for 5 minutes at 4 °C.

For the following experiment the supernatant, which was generated after the 1 000 g centrifugation step, was removed and transferred to a fresh tube. The protein concentration of the supernatant was determined by BCA protein assay. 10 µg total cell lysate protein was used as expression control (input) for western blot analysis. 250 µg of the lysate were used for Co-IP and incubated with 50 µl anti-Flag agarose beads resuspended in RIPA buffer. After an incubation period of 2 hours at 4°C using a top-over wheel, the mixture was centrifuged at 700 g for 5 minutes at 4°C. 10 µg protein of the flow through fraction were also analyzed by western blot analysis. Afterwards, the beads were washed ten times with RIPA buffer (500 µl). Following the washing steps, beads were incubated with 30 µl 1 x SDS sample puffer for 10 minutes at 99°C and centrifuged at 800 g for 5 minutes. The whole output fraction was adjusted to polyacrylamidgel-electrophoresis and western blot analysis.

## **3.7. Assays**

### **3.7.1. *In vitro* assay for triglyceride hydrolase activity**

Measurement of TG hydrolase activity of recombinant proteins is based on the release of <sup>3</sup>H-labeled oleic acid from triolein. TG substrate consisted of 1,67 mM non-radioactive triolein, 10  $\mu$ Ci <sup>3</sup>H-TO/ml and 190  $\mu$ M PC/PI (3:1). The components were mixed in an assay tube resistant to organic solvents and brought to complete dryness under a steam of nitrogen. Thereafter dried substrate was emulsified in 100 mM potassium phosphate buffer (pH 7) by sonication (three times for 30 seconds with 30 seconds pause in between). BSA was added after sonication at a final concentration of 2%. To determine TG hydrolase activity, 25  $\mu$ g COS-7 cell lysates overexpressing recombinant proteins were brought to a volume of 100  $\mu$ l with HSL buffer. Samples were incubated with 100  $\mu$ l substrate in a water bath for 1 hour at 37°C under constant shaking. As a control, incubations under identical conditions were performed with  $\beta$ -Galactosidase ( $\beta$ Gal) -expressing lysates alone. HSL buffer was used as blank. Every protein sample was measured in triplicates. After the incubation period, the reaction was terminated by adding 3,25 ml of methanol/chloroform/heptane (10/9/7) and 1 ml of 0,1 M potassium carbonate, 0,1 M boric acid (pH 10,5), and the samples were vortexed vigorously. Afterwards the samples were centrifuged at 1 000 g for 10 minutes. 200  $\mu$ l of the upper phase was transferred to a scintillation vial containing 2 ml scintillation cocktail. The radioactivity of the released FAs was measured using TRI-CARB 2300 TR liquid scintillation analyzer. To determine the specific substrate activity, 50  $\mu$ l TG substrate were measured via liquid scintillation. The activity of the substrate was determined as counts per minute (cpm/nmol FA). Activity of COS-7 cell lysates was expressed as nmol FFA/hour/mg protein.

### **3.7.2. *In vitro* assay for phospholipase activity**

Measurement of PL activity of recombinant proteins is based on the release of oleic acid from phospholipids. PL substrates consisted of 1 mM dioleoylphosphatidylcholine (dioleoyl-PC) in 100 mM potassium phosphate buffer (pH 7) and 2% BSA. Briefly, dioleoyl-PC was brought to complete dryness under

a stream of nitrogen. Thereafter dried substrate was emulsified in potassium phosphate buffer by sonication (three times for 30 seconds with 30 seconds pause in between). BSA was added after sonication.  $\beta$ -Gal containing cell lysates were used as control. HSL buffer was used as blank. Every protein sample was measured in triplicates. The release of free fatty acids was measured using the commercially available NEFA C Kit. Therefore, 80  $\mu$ l of each sample were pipetted into separate wells of a 96-well plate. Each sample was measured as duplicates. 100  $\mu$ l NEFA1 reagent were added and incubated for 10 minutes at 37°C. Afterwards 50  $\mu$ l NEFA 2 were added and incubated for another 10 minutes at 37°C. Then, the absorbance was measured at 562 nm. A NEFA standard solution (1mM) was used to generate a calibration curve.

### **3.7.3. Measurement of free fatty acids and glycerol release of cultured cells**

For the measurement of basal lipolysis, differentiated 3T3-L1 cells were incubated in 500  $\mu$ l serum free DMEM medium containing 2% BSA for 2 hours at 37°C. It is important to add BSA to the medium, because it serves as fatty acid acceptor and enables the release of fatty acids into the medium. To measure lipolysis under Forskolin-stimulated conditions, serum free DMEM medium containing 2% BSA was supplemented with 0,02 mM Forskolin. The medium was removed after each incubation period and transferred to a new 12-well plate.

The release of FFAs was measured using the commercially available NEFA C Kit. Briefly, 20  $\mu$ l of medium were pipetted into separate wells of a 96-well plate. Each sample was measured as duplicates as previously described (3.7.3. Measurement of free fatty acids and glycerol release of cultured adipocytes).

The release of glycerol into the medium was measured using the commercially available Free Glycerol Determination Kit. 30  $\mu$ l medium were pipetted in separate wells of a 96-well plate. Each sample was measured as duplicates. 100  $\mu$ l glycerol reagent was added and incubated for 10 minutes at 37°C. The absorbance was measured at 562 nm. A glycerol standard solution (2,82 mM) was used for the generation of a calibration curve.

To determine the protein concentration of 3T3-L1 cells, 500 µl of lysis solution (0,1% SDS, 0,3 M NaOH) were added to each well and incubated for 2-4 hours under shaking. The protein concentration was determined by BCA protein assay using BSA as standard.

#### **3.7.4. Preparation of conditioned media containing PEDF**

To elucidate the extracellular effect of PEDF on lipolysis, differentiated 3T3-L1 cells were incubated with conditioned medium, containing PEDF. For this purpose, COS-7 cells were transfected with PEDF-Flag construct as previously described (3.3.3. Transfection and preparation of cell lysates). Since PEDF contains an N-terminal secretion peptide and hence is secreted into the medium, COS-7 medium was used to study PEDFs effect on 3T3-L1 cells. To increase the sensitivity to pro-lipolytic factors, 3T3-L1 cells were insulin starved for 4 hours. Then, 500 µl conditioned media was added to each 12-well and cells were incubated over night. After incubation the release of FFAs and glycerol was measured (see 3.7.3. Measurement of free fatty acids and glycerol release of cultured cells).

#### **3.8. Statistical analysis**

To analyze statistical significancies Student's unpaired test (two-tailed) was performed. T-test results were considered significant for  $p < 0,05$  (\*),  $p < 0,01$  (\*\*) and  $p < 0,001$  (\*\*\*) .

# 4. Results

---

#### **4.1. New potential interaction partner of PEDF**

Previous studies already reported about PEDFs ability to interact with the major triglyceride hydrolase ATGL (Chung et al. 2008). Additionally, it was proposed that binding of PEDF regulates the subcellular localization of ATGL to lipid droplets and its interaction with GOS2, the inhibitor protein of ATGL (Dai, Zhou, et al. 2013).

To move one step closer towards deciphering the mechanism of PEDFs action, Co-IP was performed to verify its interaction with ATGL and to putatively identify new potential interaction partner of PEDF. Since it is known that binding of CGI-58 is necessary for full enzymatic activity of ATGL, CGI-58 was the first candidate chosen for this protein-protein interaction studies.

For this purpose, HEK-293 cell lysates, overexpressing His-tagged candidates and PEDF-Flag, were incubated with anti-Flag agarose beads. To avoid membrane fusions and destruction of protein complexes, cells were disrupted by shear force instead of sonication. To facilitate cell disruption process, 2% NP-40 was added to the RIPA buffer. This non-ionic detergent destabilizes the hydrophobic interactions of membrane lipids and therefore enables cell lysis with a 26G syringe needle.

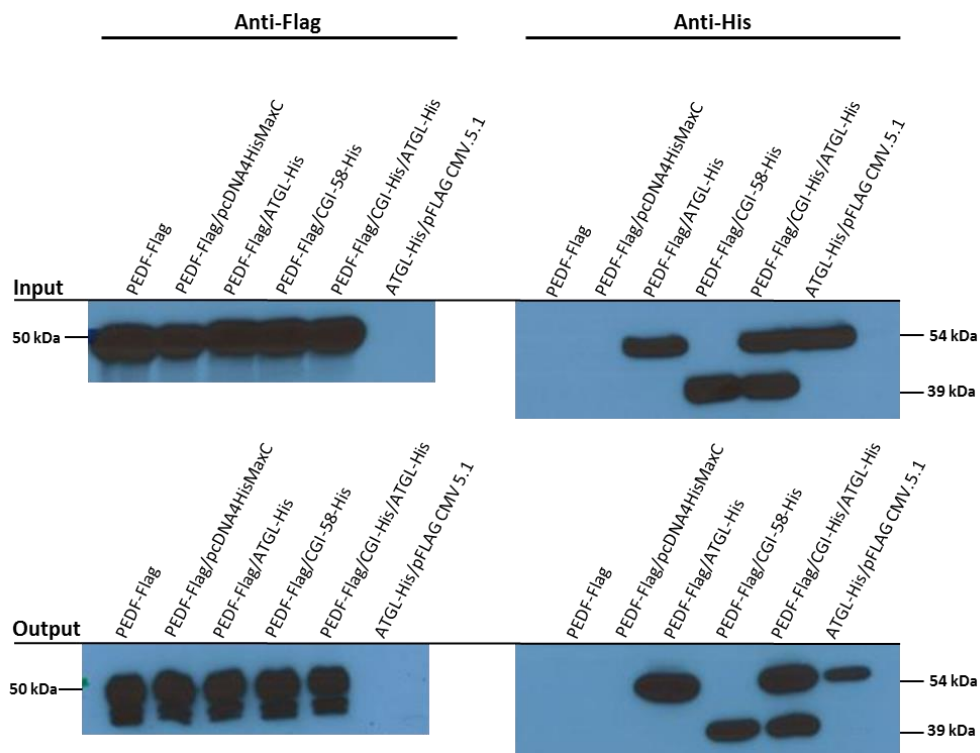


**Figure 9: Co-Immunoprecipitation revealed interaction of PEDF with CGI-58.** HEK-293 cells were transfected with PEDF-Flag and co-transfected either with PEDF-Flag/pcDNA4HisMaxC (negative control), PEDF-Flag/ATGL-His or PEDF-Flag/CGI-58-His, as well as PEDF-Flag/CGI-58-His/ATGL-His and ATGL-His/pFLAG CMV.5.1 (negative control). Cells were harvested 24 hours after transfection and disrupted in 250  $\mu$ l RIPA-Buffer containing 2% NP-40. 250  $\mu$ g lysate protein (input) were incubated with anti-FLAG-affinity gel for 3 hours at 4°C using the top-over wheel. After the incubation period, samples were washed with RIPA buffer and subsequently eluted from the anti-FLAG antibody-coupled agarose beads via 30  $\mu$ l 1 x SDS (output). 10  $\mu$ g of the input and the whole output fraction were analyzed by western blot. PEDF-Flag was detected using anti-Flag antibody conjugated with horseradish peroxidase. His-tagged proteins were detected using the anti-His polyclonal antibody and an anti-mouse True-Blot secondary antibody coupled to horseradish-peroxidase.

As shown in Figure 8, the Co-IP revealed a strong interaction of PEDF with ATGL. No unspecific binding of PEDF with the His-peptide was observed. Interestingly, PEDF also interacted with CGI-58. This result was the base for further experimental designs, including CGI-58 as a possible partner of PEDF. One problem that always occurred was a weak unspecific binding of ATGL to the Flag-peptide (see ATGL-His/pFLAG CMV.5.1).

However, the signal of the unspecific binding was much weaker compared to PEDF-Flag/ATGL-His, which indicates specific protein-protein interaction between PEDF and ATGL. To validate the interaction between PEDF and CGI-

58 further and to exclude an unspecific binding of CGI-58 to the Flag-tag of PEDF, a second Co-IP was conducted.

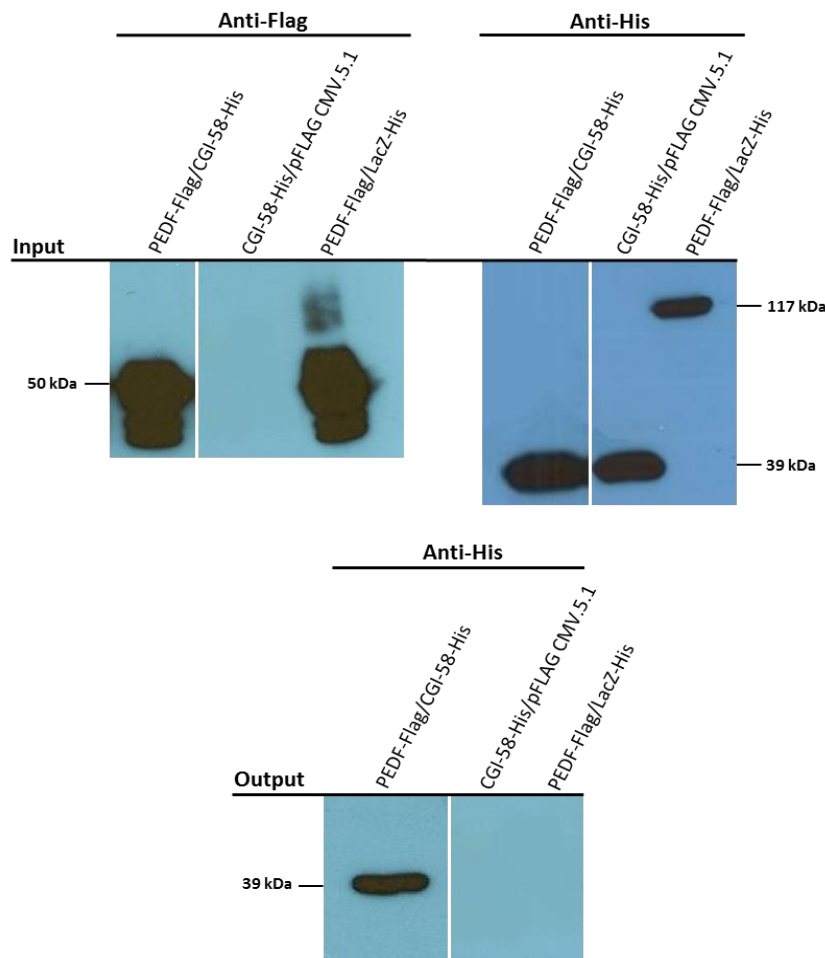


**Figure 10: Binding of CGI-58 to PEDF is independent of the Flag-tag.** HEK-293 cells were co-transfected either with PEDF-Flag/CGI-58-His (negative control), CGI-58-His/pFLAG as well as PEDF-Flag/LacZ-His (negative control). 250  $\mu$ g lysate protein was used for the incubation with anti-FLAG-affinity gel, 10  $\mu$ g of the input and 30  $\mu$ l of the output were adjusted to western blot analysis. PEDF-Flag was detected using Anti-Flag antibody conjugated with horseradish peroxidase. His-tagged proteins were detected using the anti-His polyclonal antibody and an anti-mouse True-Blot secondary antibody coupled to horseradish-peroxidase.

The result of the second Co-IP clearly demonstrated an interaction of PEDF with CGI-58, independent of the Flag-tag (see Figure 10). The negative control also showed that PEDF exhibits no general unspecific binding to proteins with a polyhistidine tag. Taken together the results indicate that CGI-58 could be a new interaction partner of PEDF in addition to ATGL.

## 4.2. Determination of TG hydrolase activity

The breakdown of TGs in adipose tissue is catalyzed by the coordinated action of ATGL, HSL and MGL. In the presence of CGI-58, ATGLs activity is increased 20-fold (Zimmermann et al. 2009).

As Co-IP experiments revealed that PEDF binds to ATGL and CGI-58, I wanted to investigate the effect of PEDF on lipolysis. It is feasible that this CGI-58-PEDF interaction is essential for PEDFs pro-lipolytic action on ATGL activity. Previous publications already reported PEDFs ability to increase lipolysis in an ATGL-dependent manner in liver and adipose tissue (Dai et al. 2013, Borg et al. 2011). Therefore it is imaginable that PEDF strengthens or facilitates the binding of CGI-58 to the patatin-domain of ATGL, thereby increasing lipolysis. Many results indicate that PEDF stimulates lipolysis, however, the exact mechanism is still unknown and therefore needs to be elucidated.

To further investigate the potential pro-lipolytic action of PEDF, *in vitro* TG hydrolase activity assays were conducted, using cell lysates prepared from transfected COS-7 cells and an artificial substrate. Since it is important for the assay that all the recombinant proteins are equally expressed, western blot analysis was performed (see Figure 11). For TG hydrolase assay His-tagged ATGL, PEDF, CGI-58 and  $\beta$ -Gal (negative control) were co-expressed in COS-7 cells.

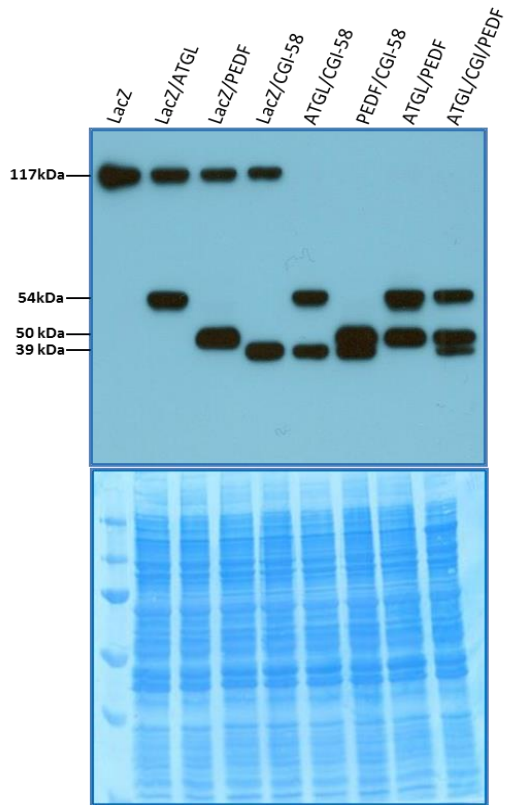


**Figure 11: Expression control of His-tagged candidates.** COS-7 cells were either transfected with LacZ-His or co-transfected with different combinations of LacZ-His, ATGL-His, PEDF-His, as well as CGI-58-His. Cells were disrupted in HSL buffer by sonication and the protein concentration was determined by Bradford protein assay. 10  $\mu$ g lysate protein were analyzed by western blot. His-tagged proteins were detected using anti-His antibody and anti-mouse-horseradish peroxidase-conjugated secondary antibody. Coomassie Blue staining of the membrane confirmed successful protein transfer and an evenly applied amount of proteins.

TG hydrolase activity assays were performed using a radiolabelled micellar TG substrate and COS-7 lysates containing overexpressed proteins.

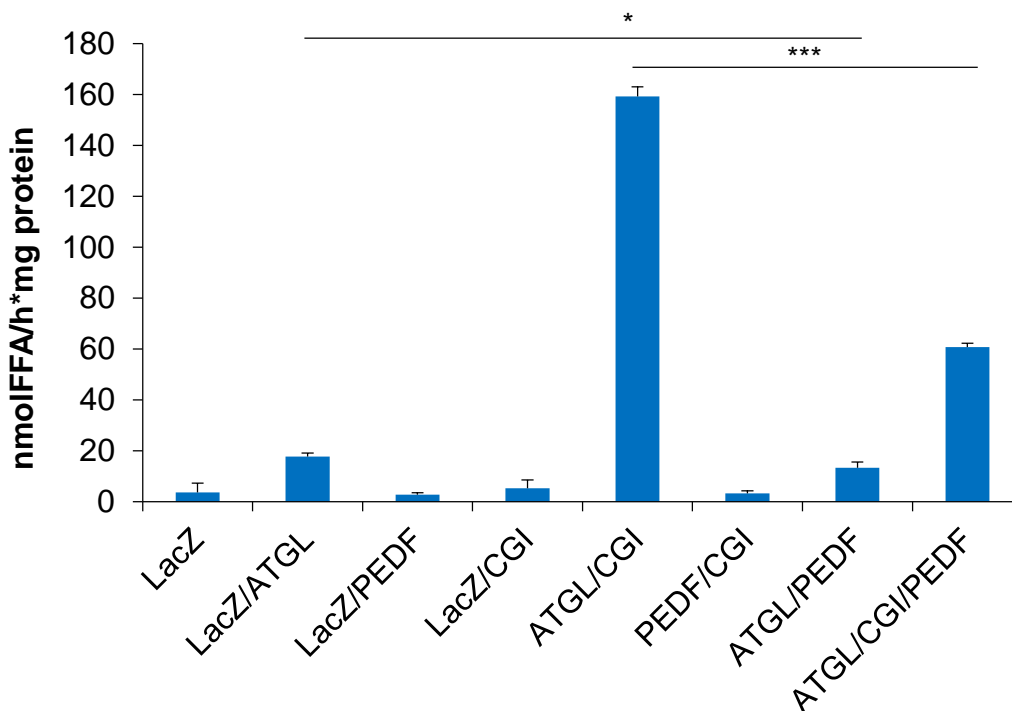


**Figure 12: PEDF has no stimulatory effect on TG hydrolase activity of ATGL.** Cytoplasmic preparations of COS-7 cells overexpressing His-tagged candidates were incubated with radioactively labeled triolein. For each reaction; 25  $\mu$ g lysate protein in 100  $\mu$ l HSL buffer were incubated for 1 hour at 37°C. The radioactively labeled FFAs were extracted and measured by liquid scintillation. Data are shown as means + standard deviation of n = 3. Statistical significance was analyzed by Student's t-test (p < 0.05 \*; p < 0.01 \*\*; p < 0.001 \*\*\*).

In accordance to previous findings, ATGL exhibits TG hydrolase activity and is stimulated by the addition of CGI-58 (~ 9-fold). Surprisingly, PEDF has no stimulatory effect on ATGL activity *in vitro*. In contrast, addition of PEDF caused a 25% decrease of ATGL activity in the absence of CGI-58 and a 62% decrease in the presence of CGI-58.

The TG hydrolase activity assay was repeated using COS-7 cell lysates containing separately expressed His-tagged candidates. The second assay was conducted to figure out whether the inhibitory effect of PEDF is dependent on intracellular effects, which only occur during co-expression of ATGL, CGI-58 and PEDF in intact cells.

Again, western blot analysis was performed to verify equal expression levels of the recombinant proteins in cell lysates (see Figure 13).

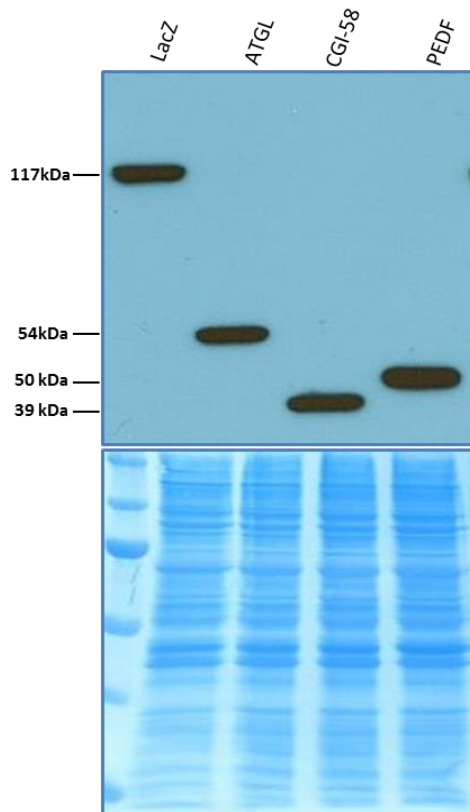


**Figure 13: Expression control of the His-tagged candidates.** COS-7 cells were transfected with LacZ-His, ATGL-His as well as CGI-58-His and PEDF-His. The cells were disrupted in HSL buffer by sonication and the protein concentration was determined using Bradford assay. 10  $\mu$ g lysate protein were analyzed by western blot. His-tagged proteins were detected using anti-His antibody and anti-mouse-horseradish peroxidase-conjugated secondary antibody. Coomassie Blue staining of the membrane confirmed successful protein transfer and an evenly applied amount of proteins

The result of the western blot shows that all His-tagged proteins were equally expressed. Additionally, the membrane was stained with Coomassie Blue to verify equal protein loading.

In contrast to the assay with co-expressed proteins, 25  $\mu$ g of each cell lysate were mixed and brought to a volume of 100  $\mu$ l with HSL buffer. Afterwards the samples were subjected to TG hydrolase assay.

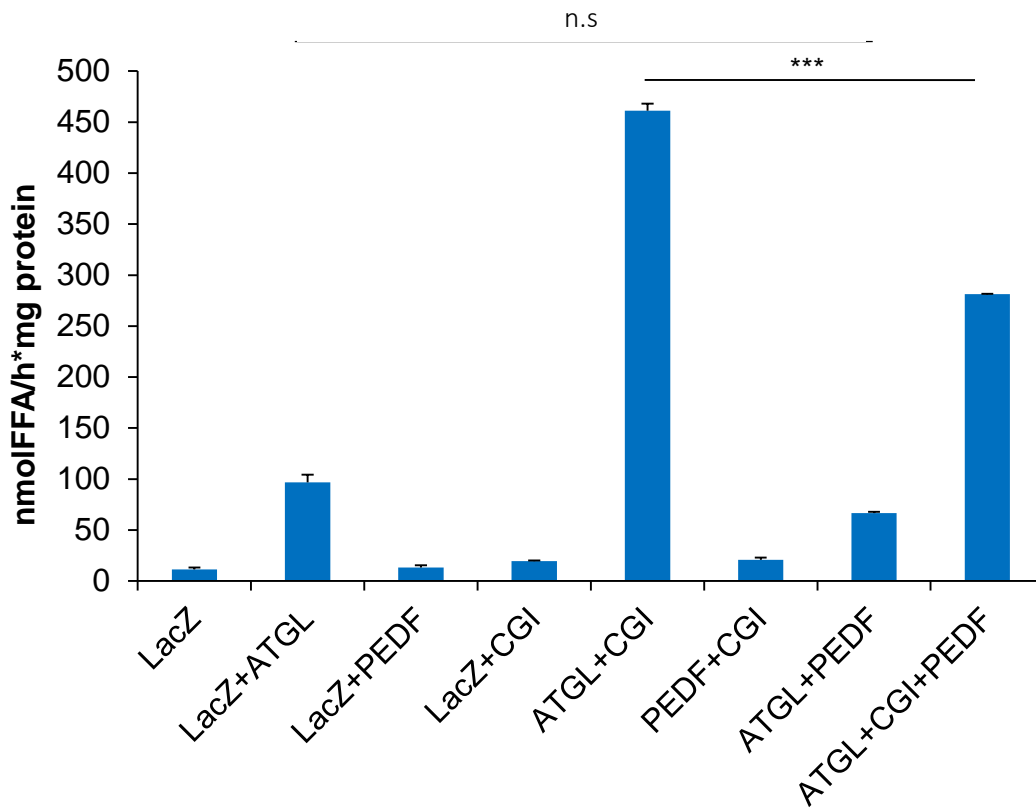


**Figure 14: PEDF shows an inhibitory effect on TG hydrolase activity of ATGL.** Cytosolic preparations of COS-7 cells overexpressing the His-tagged candidates were incubated with radioactively labeled triolein. 25  $\mu$ g of each cell lysate were mixed and solubilized in 100  $\mu$ l HSL buffer. After an incubation period of 1 hour at 37°C, radioactively labeled free fatty acids were extracted and measured by liquid scintillation cocktail. Data are shown as mean + standard deviation of n = 3. Statistical significance was analyzed by Student's t-test ( $p < 0,05$  \*;  $p < 0,01$  \*\*,  $p < 0,001$  \*\*\*).

The result of the second TG hydrolase activity assay using separately expressed proteins also revealed an inhibitory effect of PEDF on ATGL/CGI-58 mediated TG hydrolase activity (38%), however, the decrease in ATGL activity is less pronounced compared to the assay with the co-expressed candidates. Additionally, PEDF also caused a 30% decrease of basal triglyceride hydrolase activity of ATGL.

Considering the results of both assays it can be said, that PEDF caused no increase, but a decrease in TG hydrolase activity in the presence and in the absence of CGI-58.

### 4.3. Determination of phospholipase activity

Sequence alignments revealed a patatin-phospholipase-like region in ATGL, which resembles the active sites in the catalytic domains of other phospholipases. The phospholipase A<sub>2</sub> activity of ATGL is of great interest, because phospholipases are known to release bioactive FAs that function as second messengers or precursors of signal transduction mediating molecules, like eicosanoids. *Notari et al. (2006)* also reported about a potent phospholipase A<sub>2</sub> activity of ATGL, which is stimulated upon binding of the glycoprotein PEDF.

To figure out whether the addition of PEDF leads to an increase in phospholipase activity of ATGL, phospholipase activity assays were performed using Dioleoyl-PC as an artificial substrate.

For this purpose COS-7 cell lysates co-expressing His-tagged candidates (ATGL, CGI-58, PEDF and LacZ) were used. COS-7 lysates were adjusted to western blot analysis to verify equal expression (see Figure 15).

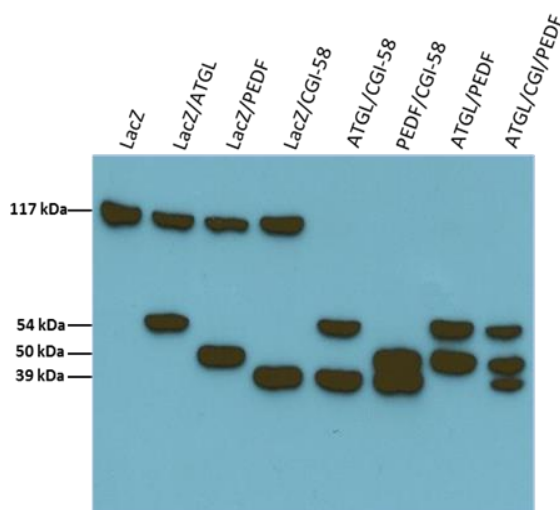


**Figure 15: Expression control of His-Tagged candidates.** COS-7 cells were either transfected with LacZ-His or co-transfected with different combinations of LacZ-His, ATGL-His, PEDF-His as well as CGI-58-His. Cells were disrupted in HSL buffer by sonication protein concentration was determined by Bradford assay. 10 µg lysate protein were used for western blot analysis. His-tagged proteins were detected using an anti-His antibody and an anti-mouse-horseradish peroxidase-conjugated secondary antibody. Coomassie Blue staining of the membrane confirmed successful protein transfer and an evenly applied amount of proteins.

As shown in Figure 15, all recombinant proteins were equally expressed. 100 µg COS-7 cell lysate protein were used for phospholipase activity assay.

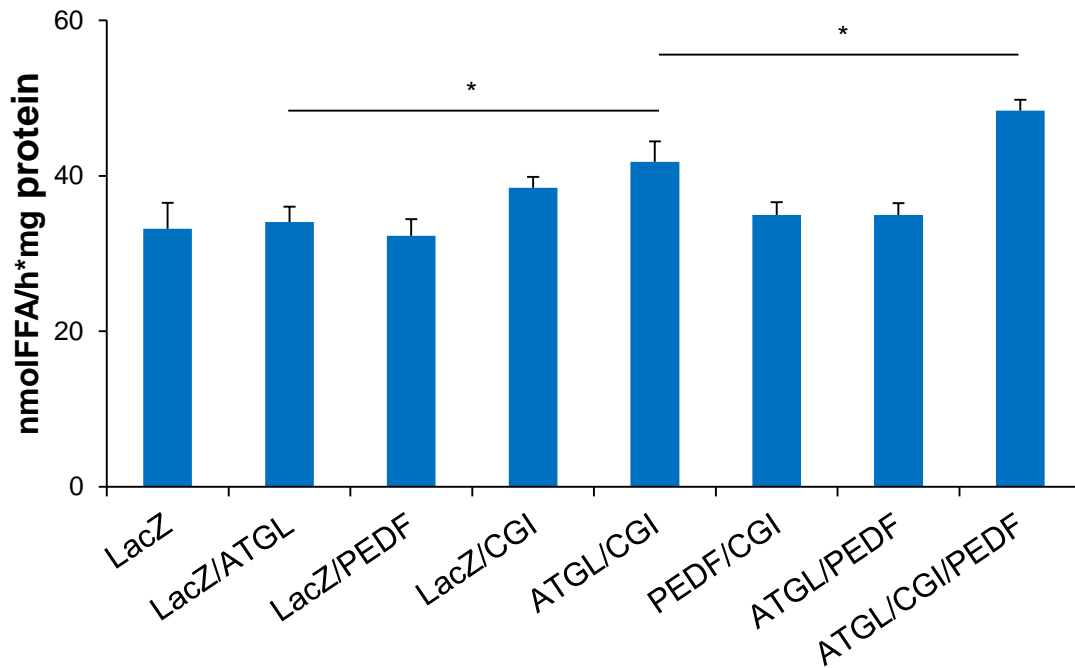


**Figure 16: Phospholipase activity of ATGL is slightly stimulated in the presence of PEDF.** Cytosolic preparations of COS-7 cells overexpressing the His-tagged candidates were analyzed for phospholipase activity using radioactively labeled phosphatidylcholine as substrate. For each reaction 100 µg lysate protein solubilized in 100 µl HSL buffer were incubated for 1 hour at 37°C. Radioactively labeled FFAs were extracted and measured by liquid scintillation. Data are shown as mean + standard deviation of n = 3. Statistical significance was analyzed by Student's t-test (p < 0,05 \*; p < 0,01 \*\*; p < 0,001 \*\*\*).

Phospholipase activity assays revealed that ATGL overexpression only slightly increased phospholipase activity of COS-7 cell lysates. This indicates that ATGL is a weak phospholipase. However, the presence of CGI-58 stimulated ATGL activity 1,2 fold, which is further significantly increased 1,4 fold by the addition of PEDF.

#### 4.4. PEDF secretion

Since it is known, that PEDF contains an N-terminal signal peptide and is secreted in high amounts from adipose tissue, I wanted to investigate whether recombinant His-tagged or Flag-tagged PEDF is also secreted from COS-7 cells.

For this purpose, COS-7 cells were transfected with recombinant constructs either encoding for PEDF harboring an N-terminal His-tag or for PEDF with a C-terminal Flag-tag. 24 hours after transfection the medium was collected and used for western blot analysis. To validate whether either of the tags is cleaved off,

medium containing PEDF was incubated with Talon-beads (anti-His) as well as Flag-affinity gel (anti-Flag). Bound proteins as well as flow through and intracellular proteins were analyzed for PEDF content using western blot techniques (see Figure 17).

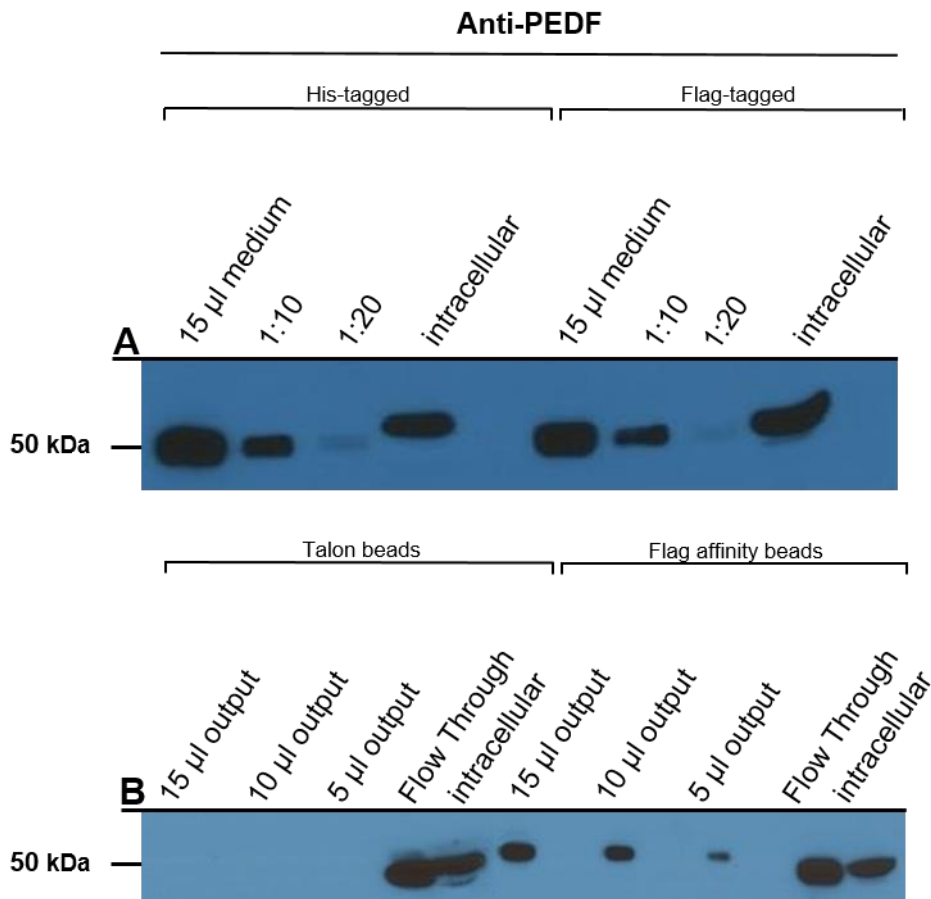


**Figure 17: Western blot analysis of PEDF secretion into COS-7 cell into medium.** **A:** 15 µl of undiluted medium and 15 µl of 1:10 and 1:20 diluted medium taken from COS-7 cells overexpressing His-tagged or Flag-tagged PEDF was analyzed for PEDF using western blot. **B:** 700 µl of medium were incubated with Talon-beads (anti-His) or with Flag-affinity gel (anti-flag). After an incubation period of 3 hours at 4°C and a centrifugation step at 700 rcf for 5 minutes, the beads were incubated for 10 minutes at 99°C with 1 x SDS. 15 µl, 10 µl and 5 µl of the undiluted output fraction were used for western blot analysis. As controls, flow through fraction as well as cell lysates were used. All proteins were detected using anti-PEDF antibody and anti-rabbit horseradish peroxidase labeled secondary antibody.

Western blot analysis clearly showed that both Flag- and His-tagged PEDF get secreted into the medium in high quantity (see Figure 17). The missing bands of His-tagged PEDF in the output fractions after Talon- purification indicate that the N-terminal polyhistidine peptide is cleaved off during secretion. This is further confirmed by the shift of the flow through band compared to intracellular PEDF,

which still contains the 6 amino acid long histidine tag. Without the N-terminal His-tag PEDF is not able to bind to the Talon-beads, with covalently attached anti-His antibodies on their surface. In comparison, the C-terminal Flag-tag is still linked with PEDF upon secretion, enabling the immunoprecipitation with anti-Flag agarose beads.

#### **4.5. Incubation of 3T3-L1 cells with PEDF containing medium**

Previous studies demonstrated that PEDF is one of the most abundant proteins released from AT (Famulla et al. 2011). For this reason it was suggested, that PEDF exerts its pro-lipolytic effect through secretion and binding to an extracellular receptor. Further indications for a ligand-receptor-dependent mechanism of PEDF was provided by *Borg et al.*. They showed that the incubation of fat pads with recombinant PEDF caused an increase in basal lipolysis, which was abolished in explants from ATGL knock out mice (Borg et al. 2011).

To investigate the extracellular effect of PEDF on differentiated adipocytes, 3T3-L1 cells were incubated with PEDF containing medium obtained from COS-7 cells overexpressing PEDF-Flag as described (4.4. PEDF secretion). As control medium obtained from untransfected COS-7 cells was used. After an incubation for 15 hours FAs and glycerol released from adipocytes was determined.

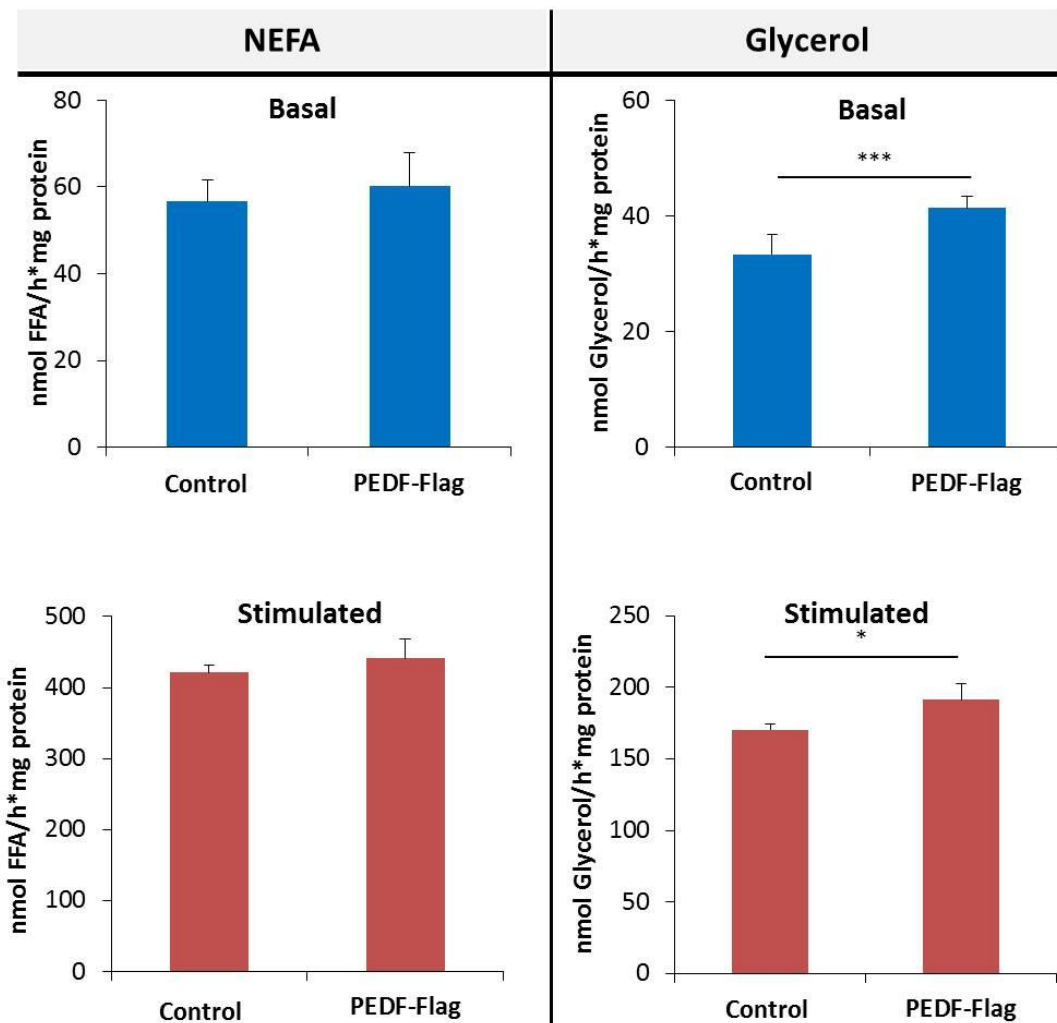


**Figure 18: Incubation of 3T3-L1 cells with PEDF containing medium increased lipolysis.** COS-7 were transfected with constructs coding for PEDF-Flag- 24 hours after transfection, the medium was collected and transferred onto differentiated 3T3-L1. After incubation, basal and Forskolin-stimulated (0,02 mM) lipolysis was measured as the release of glycerol and FFAs into the medium. Data are shown as mean + standard deviation. Statistical significance was analyzed by Student's t-test ( $p < 0,05$  \*;  $p < 0,01$  \*\*;  $p < 0,001$  \*\*\*).

Figure 18 shows that the incubation of 3T3-L1 cells with PEDF containing medium only had a minor non significant effect on FA release. In contrast, glycerol release was increased 1,2-fold in the presence of PEDF in the medium. Forskolin increases the release of FA and glycerol by 1-fold and 1,1-fold respectively. No significant effect of PEDF on stimulated FA release, but a 1,1-fold increase of stimulated glycerol was observed. It is possible that the long incubation period (15h) chosen for this experiment led to PEDF degradation.

To figure out whether PEDFs lipolytic action is based on a receptor-binding mechanism, it would be better to reduce the incubation time. For future experiments a timedependency of PEDFs effect on lipolysis is recommended.

#### 4.6. Effect of PEDF expression on differentiated 3T3-L1 cells

Recent studies revealed that plasma PEDF levels positively correlate with plasma FFAs during the progression of obesity. Furthermore it was shown that recombinant PEDF has the ability to induce basal lipolysis in cultured adipocytes (Dai et al. 2013). To further investigate the effect of PEDF expression in 3T3-L1 cells on lipolysis, a lentiviral system was used for the transduction of preadipocytes.

The lentiviral system was chosen because of its easy inducibility through withdrawal of Doxycycline and the stable expression of PEDF over a long period of time. In comparison to the adenoviral system this enables the observation of adipocyte differentiation in the presence and absence of PEDF expression.

To check whether the lentiviral system works properly, PEDF expression was analyzed by western blot analysis. For suppression of PEDF expression 1  $\mu\text{g}/\text{ml}$  Doxycycline was added to the medium. The induction of PEDF expression was induced upon removal of Doxycycline.

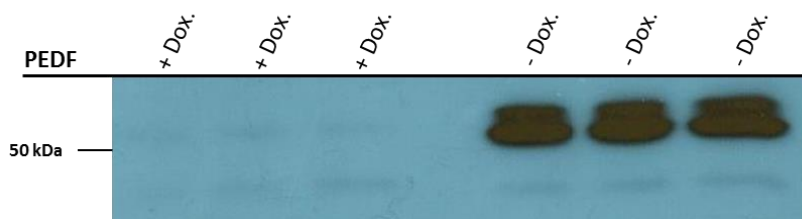


**Figure 19: PEDF expression is sufficiently repressed in the presence of Doxycycline.** Differentiated 3T3-L1 cells were disrupted in RIPA buffer containing 2% NP-40 by sonication. Protein concentration was determined vby BCA protein assay. 10  $\mu\text{g}$  of cell lysate were used for western blot analysis. PEDF was detected using an anti-PEDF polyclonal antibody and an anti-rabbit-horseradish peroxidase-conjugated secondary antibody.

The western blot showed that the expression of PEDF is efficiently suppressed by the addition of 1 µg/ml Doxycycline to the medium. In comparison, removal of Doxycycline caused a strong induction of PEDF expression in 3T3-L1 cells. Based on the result of the western blot analysis, the release of FFAs and glycerol release was determined in the presence and absence of PEDF.

To investigate the influence of intracellular PEDF on lipolysis, differentiated 3T3-L1 adipocytes were cultured with and without Doxycycline. Since PEDF expression significantly increases during adipogenesis, expression was induced at the first day of differentiation through withdrawal of Doxycycline. The control cells were always cultured in Doxycycline-containing medium. The concentration of FFAs and glycerol in the medium was determined in the basal and Forskolin-stimulated state (0,02 mM Forskolin) using commercial kits as described (3.7.3. Measurement of free fatty acids and glycerol release of cultured cells).

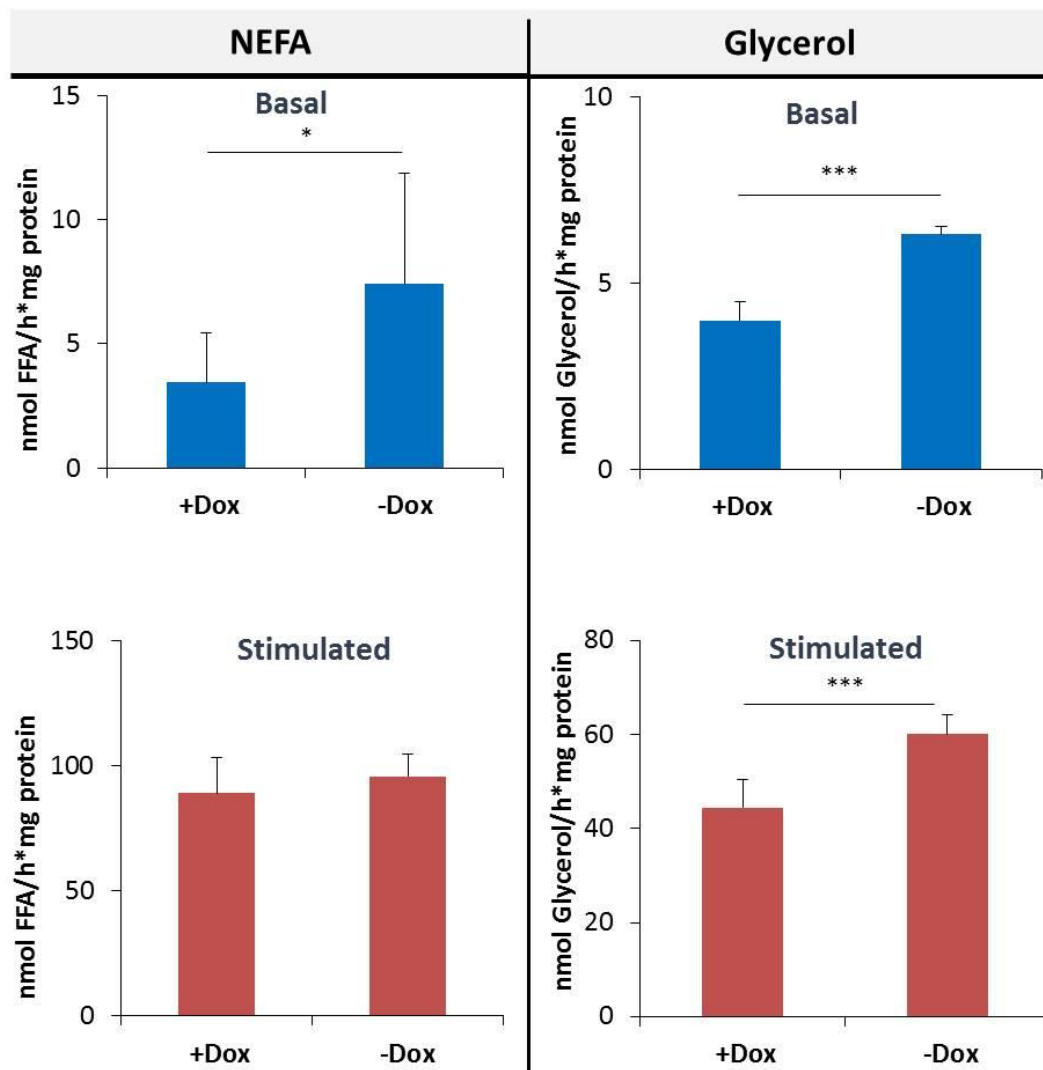


**Figure 20: Induction of PEDF expression causes a significant increase in lipolysis.** Lentiviral transduced 3T3-L1 cells were cultured in the presence or absence of Doxycycline (+/- Dox.). PEDF expression was induced on the first day of differentiation through withdrawal of Doxycycline. For determination of basal lipolysis, 3T3-L1 cells were incubated with medium containing 2% BSA for 2 hours. Afterwards the cells were incubated for 1 hour with medium containing 2% BSA and 0,02 mM Forskolin for the measurement under stimulated conditions. The concentration of NEFA (non-esterified fatty acids) and glycerol was measured using commercial kits. Data are shown as means + standard derivation. Statistical significance was analyzed by Student's t-test ( $p < 0,05$  \*;  $p < 0,01$  \*\*;  $p < 0,001$  \*\*\*).

As shown in Figure 20, PEDF expression in differentiated 3T3-L1 cells caused an increased release of FFAs (2-fold) in the basal but not in the Forskolin-stimulated state.

In comparison, the glycerol release was significantly elevated upon PEDF expression under basal as well as under Forskolin-stimulated conditions 1,6-fold and 1,3-fold respectively. Due to low levels of glycerol-3-kinase activity in

adipocytes, an enzyme responsible for the generation of glycerol-3-phosphate from glycerol, all glycerol generated during the course of lipolysis is secreted into the medium. In contrast, FAs are readily reesterified to a glycerol backbone generated during glyceroneogenesis from glucose.

Hence, the measurement of glycerol is a more reliable readout for lipolysis. Taken together this indicates that PEDF has the potential to stimulate lipolysis in cultured adipocytes.

It is known, that several intracellular phosphorylation events are necessary for the stimulation of lipolysis. To figure out whether PEDF expression causes increased activation of lipolytic key enzymes, western blot analysis of transduced 3T3-L1 cells was performed.

#### **4.7. Western blot analysis of key enzymes in lipolysis**

It is well known, that several phosphorylation steps are necessary for the full activation of lipolytic enzymes involved in TG degradation. In this process, cytosolic PKA represents the central hub of the regulatory cascade, initiating the activation of key lipolytic enzymes.

In adipocytes, lipolysis is mainly stimulated through PKA-mediated phosphorylation of HSL and PLIN1. Binding of catecholamines induces AC-mediated increase in intracellular cAMP levels, leading to the activation of PKA. Since PKA activity is dependent on the presence of this second messenger, degradation of cAMP correlates PKA activity (Holm 2003, Zechner et al. 2009).

Based on this, the influence of PEDF expression on the phosphorylation state of PKA and HSL was investigated in 3T3-L1 cells. The ATGL expression levels were also analyzed due to the positive correlation with stimulated lipolysis. For this purpose, transduced 3T3-L1 cells were harvested and disrupted by sonication in RIPA buffer. 10 µg of each cell lysate was adjusted to polyacrylamide-gel-electrophoresis for western blot analysis.

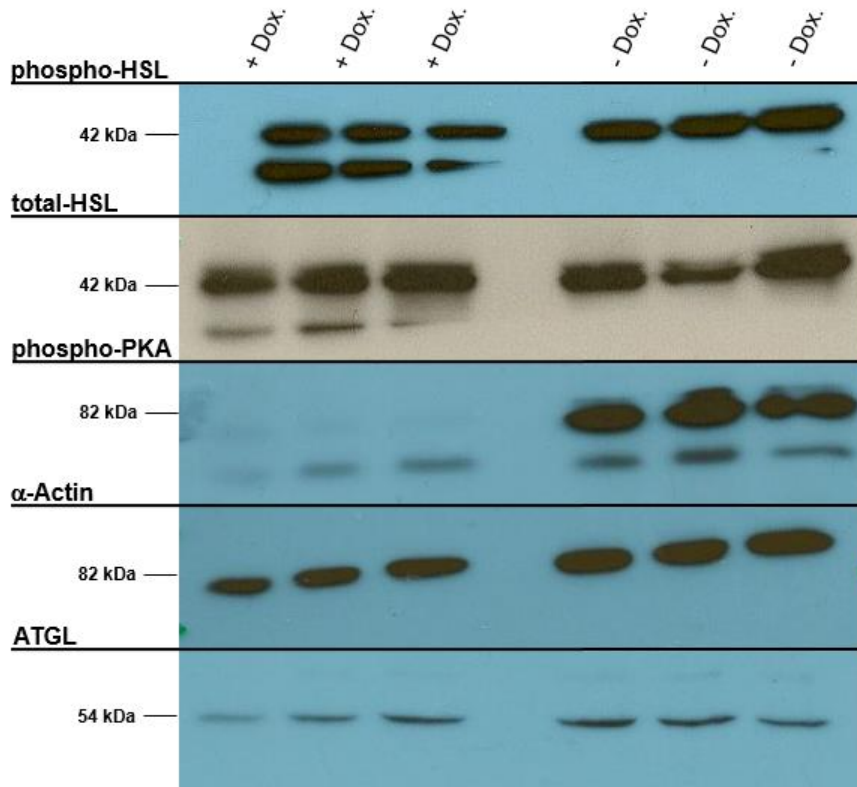


**Figure 21: Induction of PEDF expression causes increased phosphorylation of PKA and HSL.** Differentiated 3T3-L1 cells were disrupted in RIPA buffer containing 2% NP-40 by sonication. Protein concentration was determined by BCA protein assay. 10  $\mu$ g of cell lysate were used for western blot analysis. HSL was detected using anti-phospho or anti-HSL polyclonal antibody. PKA was detected with anti-phospho-PKA polyclonal antibody. Anti- $\alpha$ -actin and anti-ATGL polyclonal antibodies were used for the detection of actin and ATGL. Anti-rabbit-horseradish peroxidase-labeled secondary antibody was used for all primary antibodies.

The western blot shows that PEDF expression leads to a minor increase in HSL phosphorylation (see Figure 21). As HSL phosphorylation levels correlate with the lipolytic rate, these data indicate that PEDF stimulates lipolysis via HSL up-regulation.

Consistent with increased HSL phosphorylation status of HSL, induction of PEDF expression in 3T3-L1 adipocytes caused a marked activation of PKA, represented by its phosphorylation. This result further supports the potential pro-lipolytic action of PEDF and indicates that PEDF functions via a PKA-dependent pathway.

As shown in Figure 21, PEDF expression causes a slight increase in ATGL expression, indicating that PEDF has no positive effect on ATGL expression levels.



# 5. Discussion

---

PEDF is a multifunctional protein, shown to be involved in apoptosis, differentiation, angiogenesis and inflammatory processes. Recent studies also found a close connection between PEDF and lipid metabolism. Studies with PEDF null mice revealed a nearly twofold increase in liver TG content compared to matched wild-type animals. Consistent with this finding, prolonged administration of recombinant PEDF to PEDF-deficient mice caused a significant decrease in TG levels. Since PEDF administration causes a raise in plasma FFAs, it is feasible that PEDF has a compensatory effect for handling elevated triglyceride levels (Crowe et al., 2009, Chung et al., 2008). Hence, PEDF administration over a long period of time also changes whole-body insulin sensitivity and insulin-stimulated glucose uptake into skeletal muscle (Crowe et al. 2009). These observations were also confirmed by clinical studies, showing an up-regulation of circulating PEDF in individuals with metabolic syndrome and type II diabetes (Yamagishi et al., 2006, Crowe et al., 2009).

In 2006 *Notari et al.* identified ATGL as a potential receptor for PEDF by means of a two-hybrid system. Mutational studies with truncated versions of ATGL showed that PEDF binds to the C-terminal part of ATGL and also facilitates the translocation of the ATGL/G0S2 complex to the lipid droplet surface under stimulates conditions (Dai, Zhou, et al. 2013). However, so far it is not clear how PEDF influences lipid metabolism.

The first aim of my study was to confirm the interaction of PEDF with ATGL and to identify new potential interaction partners involved in the lipolytic process. For this purpose, we performed co-immunoprecipitation studies using HEK-293 cell lysates overexpressing PEDF, ATGL and CGI-58. Despite weak unspecific binding of ATGL to the Flag-peptide, ATGL and PEDF also exhibited a Flag-independent interaction. Since CGI-58 is the main activator of ATGL, further experiments were conducted, including CGI-58 as a possible mediator of PEDFs action.

To investigate the potential of PEDF to stimulate TG hydrolase activity of ATGL *in vitro*, TG hydrolase activity assays were performed. This assay was conducted to figure out whether PEDF stimulates lipolysis in the presence of ATGL/CGI-58. As PEDF revealed a specific interaction with CGI-58, we hypothesized that this

may contribute to PEDFs pro-lipolytic action. Against our expectations the results of the TG hydrolase assay using co-expressed candidates displayed a significant decrease (~ 62%) of ATGL/CGI-58 mediated TG hydrolase activity in the presence of PEDF. This indicates that PEDF rather has an inhibitory than a stimulatory effect *in vitro*.

To verify whether separate expression increases or decreases PEDFs inhibitory influence, COS-7 cell lysates with separately expressed candidates were mixed and subjected to TG hydrolase assay. Although the reduction of ATGL activity was less pronounced compared to the assay with the co-expressed candidates, PEDF also reduced ATGL activity up to 38%. In line with the results of the previous TG hydrolase assay, PEDF also decreased ATGL activity in the absence of CGI-58 overexpression. Since the Co-IP identified CGI-58 as a potential interaction partner, it is feasible that PEDF-bound CGI-58 is unable to bind to the patatin domain of ATGL and therefore to stimulate the enzymatic activity *in vitro*. It is reasonable to assume that ATGL and PEDF compete for the binding to CGI-58 explaining reduced CGI-58 stimulated ATGL activity in the presence of PEDF. An additional reason for the missing potential to stimulate lipolysis *in vitro*, could be the disruption of the cells. Since we use COS-7 cell lysates for the assay, it is conceivable that the loss of intact cellular components, like cytoskeleton or membranes with inserted receptors, is the reason for the lack of stimulation. Hence, it can be assumed that PEDF needs intact components of the cytoskeleton to exert its function.

Therefore we studied PEDFs intracellular role in lipolysis by overexpressing PEDF in 3T3-L1 adipocytes. For this purpose, 3T3-L1 cells were transduced with lentiviral construct for genomic integration and inducible expression of PEDF. The induction of PEDF expression in differentiated 3T3-L1 adipocytes significantly increased glycerol release under basal conditions. This result is in agreement with *Borg et al. (2011)*, showing that recombinant PEDF stimulates basal lipolysis in isolated AT explants. In addition to that, PEDF also promoted lipolysis under Forskolin-stimulated conditions.

Since PEDF contains an N-terminal signal peptide for secretion, it seems likely to exert its action via a ligand-receptor mechanism (Minkevich et al. 2010).

*Borg et al. (2011)* performed experiments with AT explants from wild-type mice which revealed an increase in basal lipolysis upon incubation with recombinant PEDF, which was not evident in ATGL knockout mice. This result supports an ATGL-dependent effect of PEDF on lipid metabolism. As we did not observe a direct effect of PEDF on increasing ATGL activity *in vitro*, we decided to incubate differentiated 3T3-L1 adipocytes with PEDF containing medium. After confirming PEDFs secretion from COS-7 cells into the medium, 3T3-L1 adipocytes were incubated for 15 hours with PEDF containing medium.

In the presence of PEDF we observed significant increase in glycerol release under basal and Forskolin-stimulated conditions. This result strengthened the hypothesis that PEDF exerts its effect on lipolysis extracellularly by binding to a receptor. To figure out whether this stimulatory effect is ATGL-dependent, further experiments using ATGL-deficient cells or the ATGL specific inhibitor Atglistatin need to be performed. However, receptor mediated effects often lead to a fast measurable response. Therefore shortening of the incubation period of 3T3-L1 adipocytes with PEDF containing medium from 15 hours to 30 minutes may avoid protein degradation and increases PEDFs effect. To decipher the optimal incubation period a time-dependent experiment can be conducted.

As already mentioned, changes in lipolysis are always accompanied with post-translational protein modifications, like increased PKA and HSL phosphorylation. Since the phosphorylation levels of these two enzymes correlate with the lipolytic rate, western blot analysis of 3T3-L1 adipocytes were performed. As the results show, increasing PEDF expression led to increased HSL phosphorylation, which corresponds to enhanced lipolysis in 3T3-L1 cells. More interestingly, PEDF caused a marked increase in phosphorylated PKA, suggesting that PEDF probably performs its pro-lipolytic effect by binding to a GPCR, leading to an increase in intracellular cAMP levels. In contrast to this, ATGL expression levels were only slightly increased in the presence of PEDF.

In 2006 *Notari et al.* reported ATGL as a new receptor for PEDF with potent phospholipase activity. Detailed analysis of the primary structure of ATGL led to the prediction of a transmembrane domain with two extracellular loops. It is thought that binding of extracellular PEDF to one of these loops stimulates the

PLA activity of ATGL, which then leads to the release of FFAs from eukaryotic membranes. In contrast to this study, PLA activity assays only revealed very little PLA activity of ATGL, which is not increased by PEDF. A possible reason for this contradiction could be explained by the storage of COS-7 cell lysates at -20°C. Several activity assays from *Notari et al.* demonstrated that ATGL only retained its PLA activity when stored at 4°C, but lost it immediately after storage at -20°C. Furthermore, *Notari et al.* added 0,1% NP-40 to purification and storage buffers, which were used for PLA assays. Therefore it is reasonable that this non-ionic detergent is necessary for solubilizing ATGL from the membrane in its native conformation. To verify whether the addition of 0,1% NP-40 or the storage of the cell lysates at 4°C influences PLA activity of ATGL, further experiments considering this change need to be conducted.

Taken together the results show PEDFs potential to stimulate lipolysis. Since western blot analysis revealed a strong PKA activation upon PEDF expression, it is conceivable that PEDFs action depends on the interaction with a GPCR, subsequently leading to increased AC activation. In the absence of the activating second messenger cAMP, PKA exists in its inactive holoenzymatic state. Upon AC activation intracellular cAMP levels increase, leading to the dissociation of the inactive holoenzyme (Amieux, Paul S. 2002). For this reason it would be important to identify this unknown receptor to decipher PEDFs mechanism of action. Additionally, CGI-58 was identified as new interaction partner. To further elucidate PEDFs role in the lipolytic cascade and to include CGI-58 in this model, further experiments are necessary.

# I. Abbreviations

---

AT	adipose tissue
ATGL	adipose triglyceride lipase
BCA	bicinchoninic acid
Bp	base pair
BSA	bovine serum albumin
cAMP	cyclic adenosine monophosphate
cDNA	complementary DNA
CDS	coding sequence
Ci	curie
cpm	counts per minute
DG	diglycerides
ddH <sub>2</sub> O	distilled, deionized water
DMEM	dulbecco's modified eagle medium
DMSO	dimethylsulfoxide
EDTA	ethylenediaminetetraacetic acid
FCS	fetal calf serum
FFA	free fatty acids
fw	foward
HSL	hormone-sensitive lipase
kDa	kilodalton
LD	lipid droplet
MCS	multiple cloning site
MG	monoglyceride
MGL	monoglyceride Lipase

PAGE	polyacrylamide gel electrophoresis
PBS	phosphate buffered saline
PC	phosphatidyl choline
PCR	polymerase chain reaction
PEDF	pigment epithelium-derived factor
PI	phosphatidyl inositol
PLIN	perilipin
RT	room temperature
rev	reverse
SDS	sodium dodecyl sulfate
Sec	second
TG	triglyceride

## II. References

---

- Amieux, Paul S., and G.S.M., 2002. Pka & pkg. *Annals of the New York Academy of Sciences*, 968.1, pp.75–95.
- Ausubel, F.M., Brent, R., Kingdom, R. E., Moore, D. M., Seidman, J. G., Smith, J. A. & Struhl & K., E., 1995. Current Protocols in Molecular Biology. *Current Protocols in Molecular Biology*. (John Wiley & Sons, NY).
- Becerra, S.P., 2006. Focus on molecules: pigment epithelium-derived factor (PEDF). *Experimental eye research*, 82.5, pp.739–740.
- Becerra, S.P. et al., 1995. Pigment epithelium-derived factor behaves like a noninhibitory serpin. Neurotrophic activity does not require the serpin reactive loop. *Journal of Biological Chemistry*, 270(43), pp.25992–25999.
- Becerra, S.P., 1997. Structure-function studies on PEDF. *Chemistry and biology of serpins*, pp.223–237.
- Berggreen, C. et al., 2009. Protein kinase B activity is required for the effects of insulin on lipid metabolism in adipocytes. *American journal of physiology. Endocrinology and metabolism*, 296, pp.E635–E646.
- Borg, M.L. et al., 2011. Pigment epithelium-derived factor regulates lipid metabolism via adipose triglyceride lipase. *Diabetes*, 60(5), pp.1458–66. Available at: <http://www.pubmedcentral.nih.gov/articlerender.fcgi?artid=3292318&tool=pmcentrez&rendertype=abstract> [Accessed March 19, 2014].
- Cannon, B. & Nedergaard, J., 2004. Brown adipose tissue: function and physiological significance. *Physiological reviews*, 84, pp.277–359.
- Carrell, R., 1987. The serpins: evolution and adaptation in a family of protease inhibitors. *Cold Spring Harbor Laboratory Press*, 52.
- Chakrabarti, P. et al., 2011. SIRT1 controls lipolysis in adipocytes via FOXO1-mediated expression of ATGL. *Journal of lipid research*, 52, pp.1693–1701.
- Chakrabarti, P. & Kandror, K. V., 2009. FoxO1 controls insulin-dependent adipose triglyceride lipase (ATGL) expression and lipolysis in adipocytes. *Journal of Biological Chemistry*, 284, pp.13296–13300.
- Chanarin, I. et al., 1975. Neutral-lipid storage disease: a new disorder of lipid metabolism. *British medical journal*, 1(March), pp.553–555.
- Chung, C. et al., 2008. Anti-angiogenic pigment epithelium-derived factor regulates hepatocyte triglyceride content through adipose triglyceride lipase (ATGL). *Journal of hepatology*, 48(3), pp.471–8. Available at: <http://www.sciencedirect.com/science/article/pii/S0168827807006265> [Accessed December 17, 2014].

- Cinti, S., 2001. The adipose organ: morphological perspectives of adipose tissues. *The Proceedings of the Nutrition Society*, 60, pp.319–328.
- Coffin, J. M. & Varmus, H. E., E., 1996. Retroviruses. *Cold Spring Harbor Laboratory Press, NY*.
- Collins, S., Cao, W. & Robidoux, J., 2004. Learning new tricks from old dogs: beta-adrenergic receptors teach new lessons on firing up adipose tissue metabolism. *Molecular endocrinology (Baltimore, Md.)*, 18(March), pp.2123–2131.
- Cornaciu, I. et al., 2011. The minimal domain of adipose triglyceride lipase (ATGL) ranges until leucine 254 and can be activated and inhibited by CGI-58 and G0S2, respectively. *PLoS ONE*, 6(10), pp.0–10.
- Cos-7.com, COS-7 cell line. <http://www.cos-7.com/>.
- Crowe, S. et al., 2009. Pigment epithelium-derived factor contributes to insulin resistance in obesity. *Cell metabolism*, 10(1), pp.40–7. Available at: <http://www.sciencedirect.com/science/article/pii/S1550413109001594> [Accessed March 6, 2015].
- Dai, Z., Qi, W., et al., 2013. Dual regulation of adipose triglyceride lipase by pigment epithelium-derived factor: a novel mechanistic insight into progressive obesity. *Molecular and cellular endocrinology*, 377(1-2), pp.123–34. Available at: <http://www.sciencedirect.com/science/article/pii/S0303720713002840> [Accessed December 28, 2014].
- Dai, Z., Zhou, T., et al., 2013. Intracellular pigment epithelium-derived factor contributes to triglyceride degradation. *The international journal of biochemistry & cell biology*, 45(9), pp.2076–86. Available at: <http://www.sciencedirect.com/science/article/pii/S1357272513002318> [Accessed December 28, 2014].
- Dawson, D.W., 1999. Pigment epithelium-derived factor: a potent inhibitor of angiogenesis. *Science*, 285.5425, pp.245–248.
- Degerman, E. et al., 1998. Phosphorylation and activation of hormone-sensitive adipocyte phosphodiesterase type 3B. *Methods (San Diego, Calif.)*, 14, pp.43–53.
- Duncan, R.E. et al., 2010. Characterization of desnutrin functional domains: critical residues for triacylglycerol hydrolysis in cultured cells. *Journal of lipid research*, 51, pp.309–317.
- Egan, J.J. et al., 1992. Mechanism of hormone-stimulated lipolysis in adipocytes: translocation of hormone-sensitive lipase to the lipid storage droplet. *Proceedings of the National Academy of Sciences of the United States of America*, 89(September), pp.8537–8541.
- Famulla, S. et al., 2011. Pigment epithelium-derived factor (PEDF) is one of the most abundant proteins secreted by human adipocytes and induces insulin resistance and inflammatory signaling in muscle and fat cells. *International journal of obesity (2005)*, 35(6), pp.762–72. Available at: <http://www.ncbi.nlm.nih.gov/pubmed/20938440> [Accessed November 6, 2014].

- Fernández-Barral, A. et al., 2014. Regulatory and functional connection of microphthalmia-associated transcription factor and anti-metastatic pigment epithelium derived factor in melanoma. *Neoplasia (New York, N.Y.)*, 16(6), pp.529–42. Available at: <http://www.pubmedcentral.nih.gov/articlerender.fcgi?artid=4198745&tool=pmcentrez&rendertype=abstract> [Accessed January 9, 2015].
- Filleur, S.Filleur, S. (2009). Characterization of PEDF: a multi - functional serpin family protein. *Journal of Cellular Biochemistry*, 106.5, 769–775., 2009. Characterization of PEDF: a multi - functional serpin family protein. *Journal of cellular biochemistry*, 106.5, pp.769–775.
- FLIER, J., 2004. Obesity WarsMolecular Progress Confronts an Expanding Epidemic. *Cell*, 116(2), pp.337–350. Available at: <http://www.sciencedirect.com/science/article/pii/S009286740301081X> [Accessed March 6, 2015].
- Fredrikson, 1986. No Title.
- Froesch, E.R., 1965. Insulin inhibition of spontaneous adipose tissue lipolysis and effects upon fructose and glucose metabolism. *Molecular pharmacology*, 1.3, pp.280–296.
- Ghosh, A.K. et al., 2008. CGI-58, the causative gene for Chanarin-Dorfman syndrome, mediates acylation of lysophosphatidic acid. *Journal of Biological Chemistry*, 283(36), pp.24525–24533.
- Granneman, J.G. et al., 2007. Analysis of lipolytic protein trafficking and interactions in adipocytes. *Journal of Biological Chemistry*, 282(8), pp.5726–5735.
- Granneman, J.G. et al., 2009. Perilipin controls lipolysis by regulating the interactions of AB-hydrolase containing 5 (Abhd5) and adipose triglyceride lipase (Atgl). *Journal of Biological Chemistry*, 284(50), pp.34538–34544.
- Greenberg, A.S. et al., 1991. Perilipin, a major hormonally regulated adipocyte-specific phosphoprotein associated with the periphery of lipid storage droplets. *Journal of Biological Chemistry*, 266(17), pp.11341–11346.
- Gruber, A. et al., 2010. The N-terminal region of comparative gene identification-58 (CGI-58) is important for lipid droplet binding and activation of adipose triglyceride lipase. *Journal of Biological Chemistry*, 285(16), pp.12289–12298.
- Gustafson, B. et al., 2009. Inflammation and impaired adipogenesis in hypertrophic obesity in man. *AJP: Endocrinology and Metabolism*, 297, pp.E999–E1003.
- Haemmerle, G. et al., 2002. Hormone-sensitive lipase deficiency in mice causes diglyceride accumulation in adipose tissue, muscle, and testis. *Journal of Biological Chemistry*, 277(7), pp.4806–4815.
- Haemmerle, G. et al., 2006. Triglyceride Lipase. , 211(May), pp.734–737.
- HEK293.com, HEK-293 cell line. <http://www.hek293.com/>.

- Hirschberg, H.J.H.B. et al., 2001. Cloning, expression, purification and characterization of patatin, a novel phospholipase A. *European Journal of Biochemistry*, 268(19), pp.5037–5044.
- Holm, C., 2003. Molecular mechanisms regulating hormone-sensitive lipase and lipolysis. *Biochemical Society transactions*, 31, pp.1120–1124.
- Huber, R., and C.R.W., 1989. Implications of the three-dimensional structure of  $\alpha$ -1-antitrypsin for structure and function of serpins. *Biochemistry*, 28.23, pp.8951–8966.
- Jenkins, A.J., 2007. Increased serum pigment epithelium - derived factor is associated with microvascular complications, vascular stiffness and inflammation in Type 1 diabetes. *Diabetic Medicine*, 24.12, pp.1345–1351.
- Jenkins, C.M. et al., 2004. Identification, cloning, expression, and purification of three novel human calcium-independent phospholipase A2 family members possessing triacylglycerol lipase and acylglycerol transacylase activities. *Journal of Biological Chemistry*, 279, pp.48968–48975.
- Jocken Johan, 2008. Adipose triglyceride lipase (ATGL) expression in human skeletal muscle is type I (oxidative) fiber specific. *Histochemistry and cell biology*, 129.4, pp.535–538.
- Joham, A.E. et al., 2012. Pigment Epithelium-Derived Factor, Insulin Sensitivity, and Adiposity in Polycystic Ovary Syndrome: Impact of Exercise Training. *Obesity*, 20(12), pp.2390–2396. Available at: <http://dx.doi.org/10.1038/oby.2012.135/nature06264>.
- Kershaw, E.E., 2013. Original Article. , 55(January), pp.1–10.
- Kershaw, E.E. & Flier, J.S., 2014. Adipose Tissue as an Endocrine Organ. *Cellular Endocrinology in Health and Disease*, 89(March), pp.229–237.
- Klingenspor, M., 2003. Cold-induced recruitment of brown adipose tissue thermogenesis. *Experimental physiology*, 88.01, pp.141–148.
- Kobayashi, K. et al., 2008. The lack of the C-terminal domain of adipose triglyceride lipase causes neutral lipid storage disease through impaired interactions with lipid droplets. *Journal of Clinical Endocrinology and Metabolism*, 93(March), pp.2877–2884.
- Kohn, A.D. et al., 1996. Expression of a constitutively active Akt Ser/Thr kinase in 3T3-L1 adipocytes stimulates glucose uptake and glucose transporter 4 translocation. *Journal of Biological Chemistry*, 271(49), pp.31372–31378.
- Kolditz, C.-I. & Langin, D., 2010. Adipose tissue lipolysis. *Current Opinion in Clinical Nutrition & Metabolic Care*, 13.4, pp.377–381.
- Lafontan, M. & Berlan, M., 1993. Fat cell adrenergic receptors and the control of white and brown fat cell function. *Journal of lipid research*, 34, pp.1057–1091.

- Lafontan, M. & Langin, D., 2009. Lipolysis and lipid mobilization in human adipose tissue. *Progress in lipid research*, 48(5), pp.275–97. Available at: <http://www.ncbi.nlm.nih.gov/pubmed/19464318> [Accessed October 31, 2014].
- Langin, D., 2006a. Adipose tissue lipolysis as a metabolic pathway to define pharmacological strategies against obesity and the metabolic syndrome. *Pharmacological research : the official journal of the Italian Pharmacological Society*, 53(6), pp.482–91. Available at: <http://www.sciencedirect.com/science/article/pii/S1043661806000478> [Accessed February 12, 2015].
- Langin, D., 2006b. Control of fatty acid and glycerol release in adipose tissue lipolysis. *Comptes Rendus - Biologies*, 329, pp.598–607.
- Lass, A. et al., 2006. Adipose triglyceride lipase-mediated lipolysis of cellular fat stores is activated by CGI-58 and defective in Chanarin-Dorfman Syndrome. *Cell Metabolism*, 3(May), pp.309–319.
- Lefèvre, C. et al., 2001. Mutations in CGI-58, the gene encoding a new protein of the esterase/lipase/thioesterase subfamily, in Chanarin-Dorfman syndrome. *American journal of human genetics*, 69, pp.1002–1012.
- Masoodi, M. et al., 2014. Lipid signaling in adipose tissue: Connecting inflammation & metabolism. *Biochimica et Biophysica Acta (BBA) - Molecular and Cell Biology of Lipids*. Available at: <http://linkinghub.elsevier.com/retrieve/pii/S1388198114002091> [Accessed October 13, 2014].
- Minkevich, N.I., Lipkin, V.M. & Kostanyan, I.A., 2010. PEDF – A Noninhibitory Serpin with Neurotrophic Activity. , 2(6), pp.62–71.
- Montero-Moran, G. et al., 2010. CGI-58/ABHD5 is a coenzyme A-dependent lysophosphatidic acid acyltransferase. *Journal of lipid research*, 51, pp.709–719.
- Neb.com, 2014, No Title. *Cloning and Synthetic Biology*.
- Nielsen, T.S. et al., 2014. Dissecting adipose tissue lipolysis: molecular regulation and implications for metabolic disease. *Journal of molecular endocrinology*, 52(3), pp.R199–222. Available at: <http://www.ncbi.nlm.nih.gov/pubmed/24577718> [Accessed December 2, 2014].
- Notari, L. et al., 2006. Identification of a lipase-linked cell membrane receptor for pigment epithelium-derived factor. *The Journal of biological chemistry*, 281(49), pp.38022–37. Available at: <http://www.ncbi.nlm.nih.gov/pubmed/17032652> [Accessed October 16, 2014].
- Ortego, J. et al., 1996. Gene expression of the neurotrophic pigment epithelium-derived factor in the human ciliary epithelium: Synthesis and secretion into the aqueous humor. *Investigative Ophthalmology and Visual Science*, 37(13), pp.2759–2767.
- Petersen, S. V, Valnickova, Z. & Enghild, J.J., 2003. Pigment-epithelium-derived factor ( PEDF ) occurs at a physiologically relevant concentration in human blood : purification and characterization. , 206, pp.199–206.

- Prigge, William F., and F.G., 1971. Effects of glucagon, epinephrine and insulin on in vitro lipolysis of adipose tissue from mammals and birds. *Comparative Biochemistry and Physiology Part B: Comparative Biochemistry*, 39.1, pp.69–82.
- Reid, B.N. et al., 2008. Hepatic overexpression of hormone-sensitive lipase and adipose triglyceride lipase promotes fatty acid oxidation, stimulates direct release of free fatty acids, and ameliorates steatosis. *Journal of Biological Chemistry*, 283(19), pp.13087–13099.
- Robidoux, J., Martin, T.L. & Collins, S., 2004. Beta-adrenergic receptors and regulation of energy expenditure: a family affair. *Annual review of pharmacology and toxicology*, 44, pp.297–323.
- Rosenwald, M. & Wolfrum, C., 2014. The origin and definition of brite versus white and classical brown adipocytes. *Adipocyte*, 3(1), pp.4–9. Available at: <http://www.pubmedcentral.nih.gov/articlerender.fcgi?artid=3917931&tool=pmcentrez&rendertype=abstract>.
- Rydel, T.J., 2003. The crystal structure, mutagenesis, and activity studies reveal that patatin is a lipid acyl hydrolase with a Ser-Asp catalytic dyad. *Biochemistry*.
- Schweiger, M. et al., 2009. Neutral lipid storage disease : genetic disorders caused by mutations in adipose triglyceride lipase / PNPLA2 or CGI-58 / ABHD5. *Am J Physiol Endocrinol Metab*, 297, pp.E289–E296.
- Schweiger, M. et al., 2008. The C-terminal region of human adipose triglyceride lipase affects enzyme activity and lipid droplet binding. *The Journal of biological chemistry*, 283(25), pp.17211–17220.
- Shen, Wen-Jun, et al., 2009. Functional interaction of hormone-sensitive lipase and perilipin in lipolysis. *Journal of lipid research*, 50.11, pp.2306–2313.
- Smorlesi, a. et al., 2012. The adipose organ: White-brown adipocyte plasticity and metabolic inflammation. *Obesity Reviews*, 13(December), pp.83–96.
- Steele, F.R. et al., 1993. Pigment epithelium-derived factor: neurotrophic activity and identification as a member of the serine protease inhibitor gene family. *Proceedings of the National Academy of Sciences of the United States of America*, 90(4), pp.1526–1530.
- Strålfors, P., Björgell, P. & Belfrage, P., 1984. Hormonal regulation of hormone-sensitive lipase in intact adipocytes: identification of phosphorylated sites and effects on the phosphorylation by lipolytic hormones and insulin. *Proceedings of the National Academy of Sciences of the United States of America*, 81(June), pp.3317–3321.
- Subramanian, V. et al., 2004. Perilipin A mediates the reversible binding of CGI-58 to lipid droplets in 3T3-L1 adipocytes. *Journal of Biological Chemistry*, 279, pp.42062–42071.
- Tamemoto, H., 1994. Insulin resistance and growth retardation in mice lacking insulin receptor substrate-1. *Nature*, 372, pp.182–186.

- Tombran-Tink, J. & Barnstable, C.J., 2003. PEDF: a multifaceted neurotrophic factor. *Nature reviews. Neuroscience*, 4(8), pp.628–636.
- Tombran-Tink, J. & Johnson, L. V., 1989. Neuronal differentiation of retinoblastoma cells induced by medium conditioned by human RPE cells. *Investigative Ophthalmology and Visual Science*, 30(8), pp.1700–1707.
- Vallet-Erdtmann, V. et al., 2004. The testicular form of hormone-sensitive lipase HSLtes confers rescue of male infertility in HSL-deficient mice. *Journal of Biological Chemistry*, 279, pp.42875–42880.
- Villena, J. a. et al., 2004. Desnutrin, an adipocyte gene encoding a novel patatin domain-containing protein, is induced by fasting and glucocorticoids: Ectopic expression of desnutrin increases triglyceride hydrolysis. *Journal of Biological Chemistry*, 279, pp.47066–47075.
- Wang, H. et al., 2009. Activation of hormone-sensitive lipase requires two steps, protein phosphorylation and binding to the PAT-1 domain of lipid droplet coat proteins. *Journal of Biological Chemistry*, 284(46), pp.32116–32125.
- Wang, P. et al., 2008. Plasma pigment epithelium-derived factor is positively associated with obesity in Caucasian subjects, in particular with the visceral fat depot. *European Journal of Endocrinology*, 159(6), pp.713–718.
- Wilson, P. a et al., 2006. Characterization of the human patatin-like phospholipase family. *Journal of lipid research*, 47, pp.1940–1949.
- Wolfe, R., 1987. Effect of short-term fasting on lipolytic responsiveness in normal and obese human subjects. *The American journal of physiology*, 252(2 Pt 1), pp.E189–E196.
- Wu, X., Wakefield, J. K., Liu, H. Xiao, H., Kralovics, R., Prchal, J. T. & Kappes, J.C., 2000. Development of a Novel Trans-Lentiviral Vector That Affords Predictable Safety . *Mol. Ther.*, 2, pp.47–55.
- Yamagishi, S.-I. et al., 2006. Elevated serum levels of pigment epithelium-derived factor in the metabolic syndrome. *The Journal of clinical endocrinology and metabolism*, 91(6), pp.2447–2450.
- Yamaguchi, T. et al., 2004. CGI-58 interacts with perilipin and is localized to lipid droplets: Possible involvement of CGI-58 mislocalization in Chanarin-Dorfman syndrome. *Journal of Biological Chemistry*, 279(29), pp.30490–30497.
- Yang, X. et al., 2010. The G0/G1 Switch Gene 2 Regulates Adipose Lipolysis through Association with Adipose Triglyceride Lipase. *Cell Metabolism*, 11(3), pp.194–205.
- Zebisch, K., 2012. Protocol for effective differentiation of 3T3-L1 cells to adipocytes. *Analytical biochemistry*, 425.1, pp.88–90.
- Zechner, R. et al., 2009. Adipose triglyceride lipase and the lipolytic catabolism of cellular fat stores. *Journal of lipid research*, 50(1), pp.3–21. Available at: <http://www.ncbi.nlm.nih.gov/pubmed/18952573> [Accessed March 19, 2014].

Zimmermann, R. et al., 2004. Fat mobilization in adipose tissue is promoted by adipose triglyceride lipase. *Science (New York, N.Y.)*, 306(5700), pp.1383–6. Available at: <http://www.ncbi.nlm.nih.gov/pubmed/15550674> [Accessed May 29, 2014].

Zimmermann, R. et al., 2009. Fate of fat: the role of adipose triglyceride lipase in lipolysis. *Biochimica et biophysica acta*, 1791(6), pp.494–500. Available at: <http://www.ncbi.nlm.nih.gov/pubmed/19010445> [Accessed November 4, 2014].

# III. List of figures

---

Figure 1: Schematic illustration of lipolysis.	4
Figure 2: Regulation of lipolysis.	9
Figure 3: The multiple roles of PEDF.	11
Figure 4: Predicted transmembrane structure of ATGL.	13
Figure 5: pcDNA4/HisMacX expression vector.	22
Figure 6: The pFLAG-CMV-5.1 expression plasmid.	23
Figure 7: The pLVX-Tight-Puro expression plasmid.	24
Figure 8: A schematic representation of the Tet-off Advanced system.	35
Figure 9: Co-Immunoprecipitation revealed interaction of PEDF with CGI-58.	47
Figure 10: Binding of CGI-58 to PEDF is independent of the Flag-tag.	48
Figure 11: Expression control of His-tagged candidates.	50
Figure 12: PEDF has no stimulatory effect on TG hydrolase activity of ATGL.	51
Figure 13: Expression control of the His-tagged candidates.	52
Figure 14: PEDF shows an inhibitory effect on TG hydrolase activity of ATGL.	53
Figure 15: Expression control of His-Tagged candidates.	54
Figure 16: Phospholipase activity of ATGL is slightly stimulated in the presence of PEDF.	55
Figure 17: Western blot analysis of PEDF secretion into COS-7 cell into medium.	56
Figure 18: Incubation of 3T3-L1 cells with PEDF containing medium increased lipolysis.	58
Figure 19: PEDF expression is sufficiently repressed in the presence of Doxycycline.	59
Figure 20: Induction of PEDF expression causes a significant increase in lipolysis.	61
Figure 21: Induction of PEDF expression causes increased phosphorylation of PKA and HSL.	63

## IV. List of tables

---

Table 1: Oligonucleotides used for cloning	21
Table 2: Antibodies used for western blot analysis	26
Table 3: Standard PCR reaction for gene cloning.	29
Table 4: Program for standard PCR reaction.	30
Table 5: Seeding density of different cell lines.	37